THE ASTRONOMICAL JOURNAL VOLUME 108, NUMBER 5 NOVEMBER 1994

EVOLUTION OF THE EARTH–MOON SYSTEM

JIHAD TOUMA

Canadian Institute for Theoretical Astrophysics, University of Toronto, Toronto M5S 1A7, Canada
Electronic mail: touma@chipmunk.cita.toronto.edu

JACK WISDOM

Department of Earth, Atmospheric, and Planetary Sciences, Massachusetts Institute of Technology, Cambridge, Massachusetts 02139
Electronic mail: wisdom@poincare.mit.edu

Received 1994 May 12; accepted 1994 June 28

ABSTRACT

The tidal evolution of the Earth–Moon system is reexamined. Several models of tidal friction are first compared in an averaged Hamiltonian formulation of the dynamics. With one of these models, full integrations of the tidally evolving Earth–Moon system are carried out in the complete, fully interacting, and chaotically evolving planetary system. Classic results on the history of the lunar orbit are confirmed by our more general model. A detailed history of the obliquity of the Earth which takes into account the evolving lunar orbit is presented.

1. INTRODUCTION

The history of the Earth–Moon system is of central interest and importance in planetary science, and numerous studies of the history of the lunar orbit have been undertaken [see Boss & Peale (1986) and Burns (1986) for recent reviews]. Goldreich's (1966) paper on the subject is classic and contains several key results. Of foremost importance, as the Moon approaches the Earth, the lunar orbit becomes highly inclined to the Earth's equator. This is in apparent contradiction with most scenarios for the formation of the Moon, which would naturally place the Moon initially in the equatorial plane. Of course this includes the presently in vogue scenario of the Moon having been created by a Mars sized impactor hitting the Earth. All lunar histories to date, including the Goldreich model, make strong approximations in the dynamics of the system to reduce the problem to manageable size. Our goal is to reexamine the dynamics of the Earth–Moon system under much less severe approximations.

In our quest we found it enlightening to first reexamine various tidal models in the context of a Hamiltonian reformulation of the multiply averaged theory presented by Goldreich (1966). This endeavor revealed the essential indifference of the dynamics to the particular tidal model in the class of tidal models we considered, and emphasized the importance of cross tidal interactions discovered to be important by Goldreich, but since largely forgotten.

We incorporate Darwin's 1872 model of tidal friction, as formulated by Mignard (1981), into our symplectic integration scheme for studying the rotational and orbital motion of extended bodies in the planetary n-body problem (Touma & Wisdom 1993; Wisdom & Holman 1991). We use this scheme to examine the history of the Earth–Moon system with accelerated tidal evolution. We also calculate new detailed histories of the Earth–Moon system, including the obliquity of the Earth, with realistic rates of tidal friction, over the last few million years.

2. GOLDREICH'S THEORY

Goldreich's 1966 theory of the moon is classic. Here we thoroughly reexamine the details of this work. Though we follow Goldreich's approximations, our Hamiltonian formulation of the dynamics is quite different from his formulation. Thus, this phase of our work provides a thorough independent check on his calculations. Furthermore, we use this framework for carefully examining the consequences of various tidal models.

2.1 Assumptions

Goldreich ignores planetary perturbations, as well as effects due to the changing Earth–Moon system on the orbit of the Earth–Moon system about the Sun. He assumes that the orbit of the Earth–Moon barycenter about the Sun is a fixed circular orbit. The orbit of the Moon is likewise taken to be a circular orbit, but is inclined relative to the ecliptic. The gravitational potential of the Earth is restricted to second order moments, and the Earth is assumed to be axisymmetric. The finite size of the Moon is ignored. The disturbing potential of the Sun on the Earth–Moon system is truncated after second order terms in the ratio of the Earth–Moon distance to the distance to the Sun. His theory is a multiply averaged "secular theory." The orbital period effects are first removed by averaging, motivated by the fact that the orbital time scales (month and year) are shorter than the node regression time scale (18 yr). Then motion on the nodal regression time scale is removed by averaging, motivated by the fact that the nodal regression time scale is much shorter than the time scale associated with tidal evolution. The first averaging is carried out analytically, the second averaging is carried out numerically.

2.2 Degrees of Freedom

Before deriving the equations of motion, we first note how Goldreich's assumptions reduce the number of degrees

 0004-6256/94/108(5)/1943/19/$0.90

of freedom of the problem. A realistic model will surely include in some manner the motion of all the planets, the Sun, and the rigid body motion of the Earth and the Moon. There are of course three degrees of freedom for the translational motion of each body, and three degrees of freedom for the most general rotational motion. The assumption of a fixed circular Earth–Moon orbit with respect to the sun drastically reduces the number of degrees of freedom. The Earth–Moon relative vector has three degrees of freedom. The Earth orientation has three degrees of freedom. Axisymmetry, plus principal axis rotation reduces to one the essential number of degrees of freedom in the orientation of the Earth. Assumption of a circular lunar orbit and averaging over orbital periods leaves one degree of freedom in the orbital motion. Averaging also eliminates the time dependence in the Sun's disturbing potential. Averaging over the precession time scale removes the remaining degree of freedom in the orbital motion. The sole nontrivial degree of freedom remaining is that associated with the obliquity and precession of the equinox of the Earth, which is coupled to the orbital inclination through the integrals of motion resulting from the averaging. Tidal interactions induce changes in the semimajor axis and the inclination of the lunar orbit, and affect the orientation of the Earth. Note that since the dynamics under these assumptions have essentially one degree of freedom, chaotic behavior is not a possibility.

2.3 Equations of Motion

Here we derive in detail the equations of motion used by Goldreich. We start with the full equations of motion, and then explicitly impose assumptions to reduce the problem.

The kinetic energy is the sum of the usual point mass kinetic energy for each body. The potential energy V of interaction of two bodies is the integral of the Newtonian potential over the mass distributions of the bodies involved. The Hamiltonian is the sum of the kinetic and potential energies:

$$H=\frac{1}{2}\sum_{i=0}^{n-1}\frac{p_i^2}{m_i}+\sum_{i<j}V_{ij}. \tag{1}$$

Following Goldreich, we truncate the potential energy to second order terms in the ratio of the radii of the bodies to the distances between them. At this order, the potential energy for an axisymmetric body interacting with other bodies (whether extended or not) has the form

$$V(\mathbf{x},\mathbf{s})=-\frac{Gm_1m_2}{r}\left[1-\frac{J_2R_e^2}{r^2}P_2(\cos\theta)\right], \tag{2}$$

where R_e is the equatorial radius of the extended body, r is the magnitude of the vector $\mathbf{x}$ from the center of mass of the extended body to the other mass, θ is the angle between $\mathbf{x}$ and the unit vector $\hat{\mathbf{s}}$ through the symmetry axis. Under these assumptions, the potential energy is

$$V=-\frac{Gm_0m_1}{r_{01}}\left[1-\frac{J_2R_e^2}{r_{01}^2}P_2(\cos\theta_{01})\right]-\frac{Gm_0m_2}{r_{02}}\left[1-\frac{J_2R_e^2}{r_{02}^2}P_2(\cos\theta_{02})\right]-\frac{Gm_1m_2}{r_{12}}, \tag{3}$$

where the indices 0, 1, and 2 refer to the Earth, Moon, and Sun, respectively, and interactions with other planets have been ignored.

2.3.1 Jacobi coordinates

To develop the equations further we need to choose a set of canonical variables, and develop the explicit form of the potential energy. The Jacobi coordinates separate the center of mass motion from the relative motion, and preserve the form of the kinetic energy as the sum over planets of squares of momenta divided by mass factors. We use Jacobi coordinates throughout because with them the disturbing potential depends only on the coordinates and this should ease the averaging steps. A convenient choice of the Jacobi indices appears to be in order of Earth, Moon, Sun, Mercury, Venus, Mars,... . The advantage is that the Earth–Moon relative vector will be one of the coordinates, and the rest will be close to the usual heliocentric Jacobi coordinates used in the planetary integrations.

We label the coordinates $\mathbf{x}_i$ with the index running from 0 to one less than the number of planets n. To define the Jacobi coordinates we introduce the notations

$$\mathbf{X}_j=\frac{\Sigma_{i=0}^{j}m_i\mathbf{x}_i}{\eta_j} \tag{4}$$

with

$$\eta_j=\sum_{i=0}^{j}m_j, \tag{5}$$

where m_i is the mass of body i. The interpretation is that $\mathbf{X}_j$ is the center of mass of the system of bodies with indices up to and including j. The Jacobi coordinates are simply

$$\mathbf{x}_i'=\mathbf{x}_i-\mathbf{X}_{i-1}, \tag{6}$$

for indices $0<i<n$, and

$$\mathbf{x}_0'=\mathbf{X}_{n-1}, \tag{7}$$

the barycenter of the whole system. Thus,

$$T=\frac{1}{2}\sum_{i=0}^{n-1}\frac{p_i^2}{m_i}=\frac{1}{2}\sum_{i=0}^{n-1}\frac{p_i'^2}{m_i'}, \tag{8}$$

where m_i' are the Jacobi reduced masses

$$m_i'=m_i\frac{\eta_{i-1}}{\eta_i}. \tag{9}$$

We need to express the potential energy in terms of the Jacobi coordinates. More specifically, we need an expression for $\mathbf{x}_i-\mathbf{x}_j$, and its magnitude, in terms of Jacobi coordinates. To this end, we note that

$$\mathbf{x}'_{i+1}-\mathbf{x}'_i=\mathbf{x}_{i+1}-\mathbf{x}_i-(\mathbf{X}_i-\mathbf{X}_{i-1}) \tag{10}$$

$$=\mathbf{x}_{i+1}-\mathbf{x}_i-\frac{m_i}{\eta_i}\mathbf{x}'_i\,. \tag{11}$$

Any difference can be found from these; thus, in particular

$$\mathbf{x}_i-\mathbf{x}_0=\mathbf{x}'_i+\sum_{j=1}^{i-1}\frac{m_j}{\eta_j}\mathbf{x}'_j\,. \tag{12}$$

More explicitly,

$$\mathbf{x}_1-\mathbf{x}_0=\mathbf{x}'_1\,, \tag{13}$$

$$\mathbf{x}_2-\mathbf{x}_0=\mathbf{x}'_2+\frac{m_1}{\eta_1}\mathbf{x}'_1\,, \tag{14}$$

and

$$\mathbf{x}_2-\mathbf{x}_1=\mathbf{x}'_2-\mathbf{x}'_1+\frac{m_1}{\eta_1}\mathbf{x}'_1=\mathbf{x}'_2-\frac{m_0}{\eta_1}\mathbf{x}'_1\,. \tag{15}$$

The inverse of the distance r_{02} is then

$$\frac{1}{r_{02}}=\frac{1}{r'_2}\left[1-\frac{m_1}{\eta_1}\frac{\mathbf{x}'_1\cdot\mathbf{x}'_2}{r'^2_2}+\frac{m_1^2}{\eta_1^2}\frac{r'^2_1}{r'^2_2}P_2\left(\frac{\mathbf{x}'_1\cdot\mathbf{x}'_2}{r'_1r'_2}\right)+\cdots\right]. \tag{16}$$

The inverse distance r_{12} is expanded in the small ratio r'_1/r'_2:

$$\frac{1}{r_{12}}=\frac{1}{r'_2}\left[1+\frac{m_0}{\eta_1}\frac{\mathbf{x}'_1\cdot\mathbf{x}'_2}{r'^2_2}+\frac{m_0^2}{\eta_1^2}\frac{r'^2_1}{r'^2_2}P_2\left(\frac{\mathbf{x}'_1\cdot\mathbf{x}'_2}{r'_1r'_2}\right)+\cdots\right]. \tag{17}$$

The potential energy can now be obtained by substitution. We make an approximation here and keep only the principal terms:

$$\begin{aligned}V=&-\frac{Gm_0m_1}{r'_1}\left[1-\frac{J_2R_e^2}{r'^2_1}P_2(\cos\theta'_1)\right]\\&-\frac{Gm_0m_2}{r'_2}\left[1-\frac{J_2R_e^2}{r'^2_2}P_2(\cos\theta'_2)-\frac{m_1}{\eta_1}\frac{\mathbf{x}'_1\cdot\mathbf{x}'_2}{r'^2_2}\right.\\&\left.+\frac{m_1^2}{\eta_1^2}\frac{r'^2_1}{r'^2_2}P_2\left(\frac{\mathbf{x}'_1\cdot\mathbf{x}'_2}{r'_1r'_2}\right)\right]-\frac{Gm_1m_2}{r'_2}\\&\times\left[1+\frac{m_0}{\eta_1}\frac{\mathbf{x}'_1\cdot\mathbf{x}'_2}{r'^2_2}+\frac{m_0^2}{\eta_1^2}\frac{r'^2_1}{r'^2_2}P_2\left(\frac{\mathbf{x}'_1\cdot\mathbf{x}'_2}{r'_1r'_2}\right)\right].\end{aligned} \tag{18}$$

Note that the terms proportional to $\mathbf{x}'_1\cdot\mathbf{x}'_2$ cancel, and the last two terms involving P_2 can be combined.

Explicit expressions for the J_2 terms are also needed. Again, let $\hat{\mathbf{s}}$ denote the direction to the principal axis which coincides with the symmetry axis. Then

$$\cos\theta'_1=\frac{\mathbf{x}'_1\cdot\hat{\mathbf{s}}}{r'_1} \tag{19}$$

and

$$\cos\theta'_2=\frac{\mathbf{x}'_2\cdot\hat{\mathbf{s}}}{r'_2}. \tag{20}$$

Thus,

$$P_2(\cos\theta'_1)=\frac{3}{2}\left(\frac{\mathbf{x}'_1\cdot\hat{\mathbf{s}}}{r'_1}\right)^2-\frac{1}{2}. \tag{21}$$

The Hamiltonian can now be divided into the Keplerian terms and the perturbations. The Keplerian part of the Hamiltonian for the Earth–Moon system is

$$H_{\rm K}=\frac{1}{2}\frac{p'^2_1}{m'_1}-\frac{Gm_0m_1}{r'_1}. \tag{22}$$

The Keplerian motion of the Earth–Moon system about the Sun is described by a similar Hamiltonian.

2.3.2 Delaunay variables

The Delaunay elements are a set of canonical coordinates which solve the Kepler problem. We consider a Keplerian Hamiltonian of the form

$$H_{\rm Kepler}=\frac{p^2}{2m}-\frac{\mu}{r}. \tag{23}$$

The Delaunay elements are: H, the angular momentum projected on the z space axis, the conjugate coordinate h, the ascending node of the orbit plane on the inertial reference plane, G, the magnitude of the angular momentum, the conjugate coordinate g, the angle from the ascending node to the pericenter (the argument of pericenter); the momentum L is related to the total energy, and is conjugate to the mean anomaly l. More specifically, $G=\sqrt{m\mu a(1-e^2)}$, where a and e are the semimajor axis and orbital eccentricity, $h=\Omega$, the longitude of the ascending node, $H=G\cos i$, where i is the orbital inclination, $L=\sqrt{m\mu a}$, and l is the mean anomaly.

The Keplerian Hamiltonian is

$$H_{\rm Kepler}=-\frac{\mu}{2a}=-\frac{m\mu^2}{2L^2}. \tag{24}$$

For unperturbed Keplerian motion the only variable which changes with time is the mean anomaly l, all other variables are constants of the motion. The mean motion n is

$$n=\frac{\partial H_{\rm Kepler}}{\partial L}=\frac{m\mu^2}{L^3}=\sqrt{\frac{\mu}{ma^3}}. \tag{25}$$

2.3.3 Andoyer variables

We also need to choose a set of canonical elements to describe the rotational motion of the Earth. The obvious choice is the Andoyer variables (Andoyer 1923). For the free rigid body they naturally express the conservation of the total angular momentum and of the space projection of the angular momentum. For the axisymmetric Earth the obliquity and equator will be represented by a single canonical pair of coordinates.

The Andoyer momenta are defined in terms of components of the angular momentum. The momentum H is the projection of the angular momentum on the z space axis. The angle h conjugate to H is the angle from the inertial reference longitude to the ascending node of the plane perpendicular to the total angular momentum. The angle between the angular momentum vector and the z space axis is I. Thus,

if G is the magnitude of the total angular momentum, then $H=G\cos I$. The next canonical momentum G is the magnitude of the angular momentum. The conjugate angle g is the angle between the ascending node of the angular momentum plane on the reference plane to the ascending node of the equator on the angular momentum plane. Finally, the projection of the angular momentum on the Z body axis is the momentum L, which is conjugate to the angle l between the ascending node of the equator on the angular momentum plane to the X body axis. The angle from the angular momentum vector to the Z body axis is J, so $L=G\cos J$.

In the body frame the kinetic energy of a rigid body is

$$T_{\text{Body}}=\frac{1}{2}\left(A\omega_A^2+B\omega_B^2+C\omega_C^2\right), \tag{26}$$

where A, B, and C are the principal moments of inertia, and ω_A, ω_B, and ω_C, are the projections of the spin vector on the respective principal axes. In terms of the spin components the components of the angular momentum are $L_A=A\omega_A$, $L_B=B\omega_B$, and $L_C=C\omega_C$. Thus, the rigid body kinetic energy is

$$T_{\text{Body}}=\frac{1}{2}\left(\frac{L_A^2}{A}+\frac{L_B^2}{B}+\frac{L_C^2}{C}\right). \tag{27}$$

Armed with this expression, we can directly derive the Hamiltonian for the free rigid body. Aligning the body axes with the principal axes with the C axis coinciding with the Z body axis, we have $L_C=L_Z=L=G\cos J$, $L_A=L_X=G\sin J\sin l$, and $L_B=L_Y=G\sin J\cos l$. The rigid body Hamiltonian is

$$H_{\text{Body}}=\left(\frac{G^2-L^2}{2}\right)\left(\frac{\sin^2 l}{A}+\frac{\cos^2 l}{B}\right)+\frac{L^2}{2C}, \tag{28}$$

where we have used the identity $G^2\sin^2 J=G^2-L^2$.

Note that the absence of g, H, and h from the Hamiltonian imply the conservation of G, h, and H, respectively. For an axisymmetric body with $A=B$ the Hamiltonian is also cyclic in l, implying L is conserved as well.

2.4 Earth–Moon Hamiltonian

We now put the pieces together to get the Hamiltonian governing the evolution of the Earth–Moon system. We keep only terms that affect the Earth–Moon system or the orientation of the Earth. With $\mu=Gm_0m_1$, the Hamiltonian for the Earth–Moon system is

$$\begin{aligned}H_{\text{Lunar}}=&-\frac{m_1'\mu^2}{2L_1^2}+\left(\frac{G_0^2-L_0^2}{2}\right)\left[\frac{\sin^2 l_0}{A}+\frac{\cos^2 l_0}{B}\right]+\frac{L_0^2}{2C}\\&+\frac{Gm_0m_1}{r_1'}\frac{J_2R_e^2}{r_1'^2}P_2(\cos\theta_1')\\&+\frac{Gm_0m_2}{r_2'}\frac{J_2R_e^2}{r_2'^2}P_2(\cos\theta_2')\\&-\frac{Gm_1m_2}{r_2'}\frac{m_0}{\eta_1}\frac{r_1'^2}{r_2'^2}P_2\left(\frac{\mathbf{x}_1'\cdot\mathbf{x}_2'}{r_1'r_2'}\right).\end{aligned} \tag{29}$$

The Earth–Moon orbital variables have the subscript 1, corresponding to the Jacobi index; this distinguishes them from the Andoyer variables which here have subscript 0. The first term gives the unperturbed Kepler motion of the Earth–Moon system. The second line gives the unperturbed rotational motion of the Earth. The third line gives the Moon's torque on the Earth, and the effect of the Earth's oblateness on the Earth–Moon orbit. The fourth line gives the Sun's torque on the Earth, and if the Earth–Sun orbit were allowed to vary, it would represent the effect of the oblateness of the Earth on the orbit of the Earth–Moon system about the Sun. The fifth line gives the Sun's perturbation on the Earth–Moon orbit, and if the Earth–Sun orbit was allowed to vary, it would also represent the effect of the finite size of the Earth–Moon system on the orbit of the Earth–Moon system about the Sun.

2.5 Averaging Over Orbital Time Scales

In this section we carry out the averaging over the orbital periods. At this point we incorporate Goldreich's assumption that the Earth–Moon system follows a circular orbit with respect to the Sun, and that the Earth–Moon orbit is circular. That is, we assume $r_i'=a_i$ is fixed. With this, we also assume that the mean anomaly of the Earth–Moon system evolves uniformly with time $l_i=n_it$, where the period is $2\pi/n_i$.

For principal axis rotation, the direction of the spin axis and the C body axis coincide with the direction of the angular momentum vector. The inertial components of $\hat{\mathbf{s}}$ are $\hat{s}_x=\sin I\sin h$, $\hat{s}_y=-\sin I\cos h$, $\hat{s}_z=\cos I$. We will use the relation $\cos I=H/G$, to express the interaction in terms of Andoyer variables. We have

$$r_i'\cos\theta_i'=x_i'\sin I\sin h-y_i'\sin I\cos h+z_i'\cos I. \tag{30}$$

$$\text{Using } x_2'=a_2\cos(n_2t), y_2'=a_2\sin(n_2t), \text{ and } z_2'=0,$$

$$\cos\theta_2'=\sin I\sin(h-n_2t). \tag{31}$$

The expressions for $\mathbf{x}_1'$ are more complicated because the assumed motion is out of the plane. The vector $\mathbf{x}_1'$ is obtained from the vector $(a_1\cos n_1t, a_1\sin n_1t, 0)$, by successive rotations by the orbital inclination i about the ascending node and then a rotation about the spatial z axis by the longitude of the node Ω. The result is

$$x_1'=a_1(\cos\Omega\cos n_1t-\sin\Omega\cos i\sin n_1t), \tag{32}$$

$$y_1'=a_1(\sin\Omega\cos n_1t+\cos\Omega\cos i\sin n_1t), \tag{33}$$

$$z_1'=a_1\sin i\sin n_1t. \tag{34}$$

We find

$$\begin{aligned}\cos\theta_1'=&\sin I\sin(\Omega-h)\cos n_1t\\&+[\cos I\sin i-\sin I\cos(\Omega-h)\cos i]\sin n_1t.\end{aligned} \tag{35}$$

We also need $\mathbf{x}_1\cdot\mathbf{x}_2$. We find

$$\frac{\mathbf{x}_1\cdot\mathbf{x}_2}{a_1a_2}=(\cos\Omega\cos n_1t-\sin\Omega\cos i\sin n_1t)\cos n_2t+(\sin\Omega\cos n_1t+\cos\Omega\cos i\sin n_1t)\sin n_2t. \tag{36}$$

We substitute these into the Hamiltonian and carry out the averaging over the orbital periods. At this point we also specialize to an axisymmetric Earth with $A=B$. We find

$$H_{\rm Lunar}=-\frac{m_1'\mu^2}{2L_1^2}+\frac{G_0^2-L_0^2}{2A}+\frac{L_0^2}{2C}+\frac{Gm_0m_1}{a_1}\frac{J_2R_e^2}{a_1^2}\times\left(\frac{3}{4}\{\sin^2 I\sin^2(h_0-\Omega)+[\cos I\sin i-\sin I\cos i\cos(h_0-\Omega)]^2\}-\frac{1}{2}\right)+\frac{Gm_0m_2}{a_2}\frac{J_2R_e^2}{a_2^2}\times\left(\frac{3}{4}\sin^2 I-\frac{1}{2}\right)+\frac{Gm_1m_2}{a_2}\frac{m_0}{\eta_1}\frac{a_1^2}{a_2^2}\left(\frac{3}{8}\sin^2 i-\frac{1}{4}\right). \tag{37}$$

Note that the first square bracket is the square of the sine of the mutual obliquity ϵ of the spin axis with respect to the orbit normal of the moon

$$\sin^2\epsilon=\sin^2 I\sin^2(h_0-\Omega)+[\cos I\sin i-\sin I\cos i\cos(h_0-\Omega)]^2. \tag{38}$$

It will be helpful to define some constants (keeping in mind that the constants will change when tides are incorporated). Define

$$C_1=-\frac{Gm_0m_1}{a_1}\frac{J_2R_e^2}{a_1^2}\frac{3}{4}, \tag{39}$$

$$C_2=-\frac{Gm_0m_2}{a_2}\frac{J_2R_e^2}{a_2^2}\frac{3}{4}, \tag{40}$$

and

$$C_3=-\frac{Gm_1m_2}{a_2}\frac{m_0}{\eta_1}\frac{a_1^2}{a_2^2}\frac{3}{8}. \tag{41}$$

The constants are (from Allen 1973) the mass of the Earth $m_0=5.976\times10^{27}$ g, the mass of the Moon $m_1=m_0/81.301=7.350\times10^{25}$ g, the mass of the Sun $m_2=1.989\times10^{33}$ g, the mean Earth–Moon distance $a_1=384\,400$ km, the mean Earth–Sun distance $a_2=1.495\,979\times10^{13}$ cm, the angular momentum of the Earth $G=5.861\times10^{40}$ cm^2 g s^{-1}, the oblateness of the Earth $J_2=0.001\,082\,64$, the equatorial radius of the Earth $R_e=6378.164$ km, and the gravitational constant $G=6.67\times10^{-8}$ dyn cm^2 g^{-2}. We deduce $G_1=\sqrt{m_1'Gm_0m_1a_1(1-e_1^2)}=2.8552\times10^{41}$ cm^2 g s^{-1}, using $e_1=0.0549$. In terms of these constants we can form frequencies: $\alpha_1=-2C_1/G_0=5.8139\times10^{-12}$ s^{-1}, $\alpha_2=-2C_2/G_0=2.6693\times10^{-12}$ s^{-1}, and $\alpha_3=-2C_3/G_1=1.116\,743\times10^{-8}$ s^{-1}. The corresponding periods are 34 245.80, 74 590.96, and 17.83 yr, respectively.

Using these definitions, ignoring constant terms, and writing the sines in terms of cosines, the Hamiltonian becomes

$$H_{\rm Lunar}=C_1\cos^2\epsilon+C_2\cos^2 I+C_3\cos^2 i. \tag{42}$$

Note that the three cosines correspond to Goldreich's variables: $x=\cos I$, $y=\cos i$, and $z=\cos\epsilon$. Goldreich's scalar angular momenta correspond to canonical momenta: $H=G_0$, and $h=G_1$. Up to a scale factor $H_{\rm Lunar}$ is the same as χ in Goldreich's paper. The C_i are simply related to Goldreich's constants L, K_1, and K_2: $C_1=L/2$, $C_2=K_1/2$, and $C_3=K_2/2$, taking into account Goldreich's definition of $J=3J_2/2$.

Looking ahead at this point we note that Hamilton's equations derived from this Hamiltonian will be singular when either i or I is zero, for then the nodes are not defined. For the evolution of the Moon as found by Goldreich the obliquity does not get small but the inclination of the Moon does. Thus, we only need to remove the orbit singularity. To avoid the singularity we carry out a sequence of transformations. First, it is convenient to change variables so that the momentum conjugate to the node becomes small if the inclination is small. A transformation that accomplishes this has the generating function

$$F=-h_1H_1'+(g_1+h_1)G_1'+l_1L_1'. \tag{43}$$

This gives $h_1'=-h_1$, $g_1'=g_1+h_1$, $l_1'=l_1$, but more importantly $H_1'=G_1-H_1$, $G_1'=G_1$, and $L_1'=L_1$. We have

$$H_1'=G_1-H_1=G_1(1-\cos i)=2G_1\sin^2\frac{i}{2}. \tag{44}$$

The momentum H_1' is small with small i as desired.

Next, we make use of the fact that only one combination of angles $h_0-\Omega=h_0+h_1'$ appears in the Hamiltonian. We use the generating function

$$F=(h_0+h_1')H_1''+h_0H_2''+\text{identity}, \tag{45}$$

to yield $H_1''=H_1'$ and $H_2''=H_0-H_1'=H_0+H_1-G_1$, which is conserved since the Hamiltonian does not depend on h_2''.

Having made use of the obvious integrals, we need to finish the job of removing the singularity. We define

$$x=\sqrt{2H_1''}\cos h_1''=2\sqrt{G_1}\sin\frac{i}{2}\cos(h_0-\Omega), \tag{46}$$

$$y=\sqrt{2H_1''}\sin h_1''=2\sqrt{G_1}\sin\frac{i}{2}\sin(h_0-\Omega). \tag{47}$$

The variable x is the momentum conjugate to the coordinate y.

To write the Hamiltonian in terms of x and y we first derive some intermediate results:

$$\sin i\cos(h_0-\Omega)=\frac{x}{\sqrt{G_1}}\sqrt{1-\frac{x^2+y^2}{4G_1}}, \tag{48}$$

$$\cos i=1-2\sin^2\frac{i}{2}=1-2\left(\frac{x^2+y^2}{4G_1}\right), \tag{49}$$

and

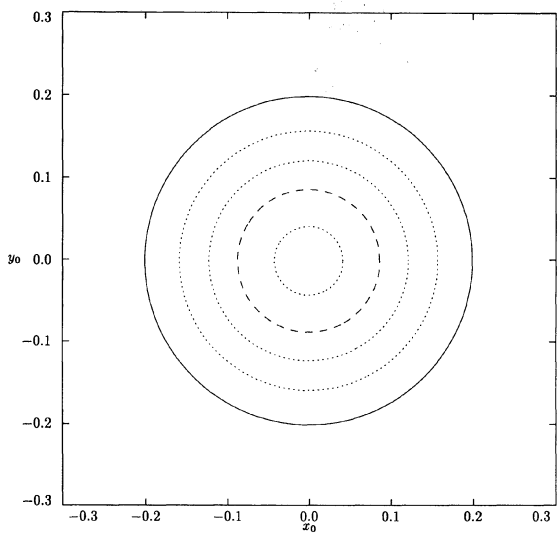

FIG. 1. The $x-y$ phase plane for the present configuration of the Earth–Moon system. The dashed line is the trajectory of the actual system. The dotted lines show other trajectories in the phase plane. The solid line is the boundary of the allowed phase plane.

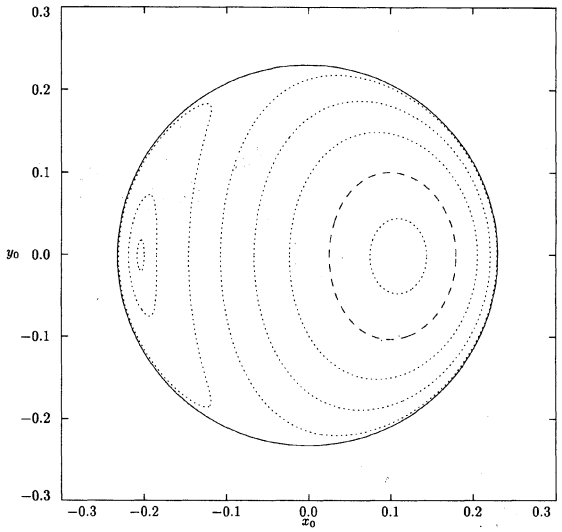

FIG. 2. The $x-y$ phase plane for the Earth–Moon system when the semi-major axis of the lunar orbit is near $5R_e$. The dashed line is the trajectory of the actual system. The dotted lines show other trajectories in the phase plane. The solid line is the boundary of the allowed phase plane.

$$\cos\epsilon=\cos i\cos I+\cos(h_0-\Omega)\sin i\sin I$$
$$=\left[1-2\left(\frac{x^2+y^2}{4G_1}\right)\right]\frac{H_0}{G_0}$$
$$+\frac{x}{\sqrt{G_1}}\sqrt{1-\frac{x^2+y^2}{4G_1}}\sqrt{1-\frac{H_0^2}{G_0^2}}. \quad (50)$$

The Hamiltonian is then

$$H_{\rm Lunar}=C_1\left\{\left[1-2\left(\frac{x^2+y^2}{4G_1}\right)\right]\frac{H_0}{G_0}\right.$$
$$\left.+\frac{x}{\sqrt{G_1}}\sqrt{1-\frac{x^2+y^2}{4G_1}}\sqrt{1-\frac{H_0^2}{G_0^2}}\right\}^2+C_2\frac{H_0^2}{G_0^2}$$
$$+C_3\left[1-2\left(\frac{x^2+y^2}{4G_1}\right)\right]^2 \quad (51)$$

with $H_0=H_2''+(x^2+y^2)/2$. The Hamiltonian is a mess, but it is not singular for $x=y=0$. Note that Goldreich must at each step determine which of the two solutions of a quadratic equation is the appropriate one to use. We have no such ambiguity here.

Before proceeding we must understand the $x-y$ phase space. Keep in mind that x and y are conjugate variables. The Hamiltonian is an even function of y so all of the trajectories are symmetrical about the x axis. There is a single fixed point for positive x with $y=0$ when the Moon is far from the Earth. For convenience we define scaled versions of x and y: $x'=x/\sqrt{G_{10}}$, and $y'=y/\sqrt{G_{10}}$, G_{10} is the value of G_1 at the present. The phase plane for the present configuration of the Earth–Moon system is shown in Fig. 1. The trajectory of the Earth–Moon system is here put in relation to other possible trajectories of the system. The phase plane shows the dynamical context in which the actual trajectory sits. To our knowledge, other treatments have not put the dynamics of the Moon in context in this way. It is especially interesting to note that when the Moon is close to the Earth there is a second fixed point with negative x with $y=0$ (Fig. 2). The constants and state variables have here been chosen self-consistently according to the evolution described below, using the complete Darwin–Mignard tides with lunar–solar cross terms. The second fixed point does not affect the evolution of our Moon, but it is interesting to see that other, qualitatively different, dynamical possibilities exist.

Note that the area on the $x-y$ phase plane is nearly conserved by the tidal evolution. The area enclosed by the system trajectory (the dashed line) in Fig. 2 is only 4 percent larger than the area enclosed by the system trajectory in Fig. 1, even though the values of the Hamiltonian and the angular momentum of the Earth and Moon have each changed by about a factor of 4 (4.585, 0.2898, 3.771, respectively). The observed difference in area is not an artifact of numerical error or the speed of tidal evolution, since the tidal time scale can be scaled out of the equations of motion. Presumably, the small difference in the areas reflects the nonadiabatic nature of the evolution with dissipation. Another possibility is that the phase plane area is only a first-order adiabatic invariant, and that a more accurate adiabatic invariant exists. We believe our observation of the near adiabatic evolution of the area on the $x-y$ phase plane is nontrivial and new.

2.6 *Tidal Equations*

In this section we develop the equations for the variation of the constants in terms of the tidal torques. For convenience, we use Goldreich's notation: $\hat{\mathbf{a}}$ is the unit vector along the spin axis, $\hat{\mathbf{b}}$ is the unit vector normal to the lunar orbit plane, and $\hat{\mathbf{c}}$ is the unit vector normal to the ecliptic. Let

$\mathbf{T}_0$ be the torque on the Earth, and $\mathbf{T}_1$ be the torque on the Moon. Of course, in the absence of solar torques we have $\mathbf{T}_0=-\mathbf{T}_1$.

Components of the tidal torques directly affect corresponding components of the angular momenta:

$$\frac{dG_0}{dt}=\mathbf{T}_0\cdot\hat{\mathbf{a}}, \tag{52}$$

$$\frac{dH_0}{dt}=\mathbf{T}_0\cdot\hat{\mathbf{c}}, \tag{53}$$

$$\frac{dG_1}{dt}=\mathbf{T}_1\cdot\hat{\mathbf{b}}, \tag{54}$$

and

$$\frac{dH_1}{dt}=\mathbf{T}_1\cdot\hat{\mathbf{c}}. \tag{55}$$

In the absence of solar torques $H_{\text{Total}}=H_0+H_1$ is constant.

The equations governing the evolution of x and y need not be modified since these will be integrated only over the precession period to carry out the averages for the longer term tidal evolution of the constants. However, if these equations were to be integrated for a long time, then tidal corrections would have to be added. Goldreich avoids computing these corrections by computing the secular tidal evolution of the Hamiltonian, and from the value of the Hamiltonian he solves for the appropriate starting conditions for the nodal precession equations (here, values of x and y). Following Goldreich, we need to develop the equations for the secular evolution of the Hamiltonian. As the evolution proceeds we solve for the value of x with $y=0$ near the previous value that has the correct value of the Hamiltonian. This is used as the initial condition in the numerical integration over the precessional period to compute the precessional averages of the tidal equations derived below.

The equations governing the evolution of the constants are simply derived. We note that a_1 is proportional to G_1^2. The moment J_2 is approximately given by

$$J_2=k_s R_e^5\Omega^2/(3GI), \tag{56}$$

where $k_s=0.947$ is a secular Love number chosen to give the known value of J_2, Ω is the angular rotation rate of the Earth, and $I=m_0R_e^2$. Recall that Ω is proportional to G_0. Thus, $C_1\propto G_0^2/G_1^6$, $C_2\propto G_0^2$, and $C_3\propto G_1^4$. We derive then

$$\frac{dC_1}{dt}=C_1\left(2\frac{\dot{G}_0}{G_0}-6\frac{\dot{G}_1}{G_1}\right)=C_1\left(2\frac{\mathbf{T}_0\cdot\hat{\mathbf{a}}}{G_0}-6\frac{\mathbf{T}_1\cdot\hat{\mathbf{b}}}{G_1}\right), \tag{57}$$

$$\frac{dC_2}{dt}=C_2\left(2\frac{\dot{G}_0}{G_0}\right)=C_2\left(2\frac{\mathbf{T}_0\cdot\hat{\mathbf{a}}}{G_0}\right), \tag{58}$$

and

$$\frac{dC_3}{dt}=C_3\left(4\frac{\dot{G}_1}{G_1}\right)=C_3\left(4\frac{\mathbf{T}_1\cdot\hat{\mathbf{b}}}{G_1}\right). \tag{59}$$

Next we develop the equations governing the tidal evolution of the three cosines: $\cos\epsilon$, $\cos I$, and $\cos i$. The latter two are easy:

$$\frac{d\cos I}{dt}=\cos I\left(\frac{\dot{H}_0}{H_0}-\frac{\dot{G}_0}{G_0}\right)=\frac{\mathbf{T}_0\cdot\hat{\mathbf{c}}-\cos I\mathbf{T}_0\cdot\hat{\mathbf{a}}}{G_0} \tag{60}$$

and

$$\frac{d\cos i}{dt}=\cos i\left(\frac{\dot{H}_1}{H_1}-\frac{\dot{G}_1}{G_1}\right)=\frac{\mathbf{T}_1\cdot\hat{\mathbf{c}}-\cos i\mathbf{T}_1\cdot\hat{\mathbf{b}}}{G_1}. \tag{61}$$

The direct derivation of the time derivative of $\cos\epsilon$ is more complicated. However, Goldreich's derivation is fairly easy to follow, and the result can be checked by a direct calculation. In our notation we have

$$\frac{d\cos\epsilon}{dt}=\frac{\mathbf{T}_0\cdot\hat{\mathbf{b}}-\mathbf{T}_0\cdot\hat{\mathbf{a}}\cos\epsilon}{G_0}+\frac{\mathbf{T}_1\cdot\hat{\mathbf{a}}-\mathbf{T}_1\cdot\hat{\mathbf{b}}\cos\epsilon}{G_1}. \tag{62}$$

Combining terms, the time derivative of the Hamiltonian is

$$\begin{aligned}\frac{dH_{\text{Lunar}}}{dt}=&2C_1\cos\epsilon\left(\frac{\mathbf{T}_0\cdot\hat{\mathbf{b}}}{G_0}+\frac{\mathbf{T}_1\cdot\hat{\mathbf{a}}}{G_1}-4\cos\epsilon\frac{\mathbf{T}_1\cdot\hat{\mathbf{b}}}{G_1}\right)\\&+2C_2\cos I\frac{\mathbf{T}_0\cdot\hat{\mathbf{c}}}{G_0}\\&+2C_3\cos i\left(\frac{\mathbf{T}_1\cdot\hat{\mathbf{c}}}{G_1}+\cos i\frac{\mathbf{T}_1\cdot\hat{\mathbf{b}}}{G_1}\right).\end{aligned} \tag{63}$$

2.7 Tidal Models

We examine the evolution with several tidal models. They include (1) the MacDonald tides, (2) the Darwin tides with constant and equal phase lags, (3) the Darwin tides with phase lags proportional to frequency, and (4) Darwin–Mignard tides. We consider the evolution with just the Earth–Moon tides, the evolution with the addition of direct solar tides, and the evolution with solar tides including solar–lunar cross terms.

The MacDonald tides model the distortion of the body as a second harmonic distortion. Friction is introduced by delaying the tide with respect to the tide raising potential. The delay is incorporated as a constant phase lag, which does not make any sense for eccentric orbits. Darwin's (1880) approach is to Fourier expand the tide raising potential and then introduce friction through phase lags in each (uniformly moving) term. A problem with this approach is that the phase lags are numerous and essentially unconstrained by observations, but the approach is more satisfying than MacDonald's approach which seems arbitrary. Mignard (1981) has developed a different formulation of the Darwin tides. In his formulation the distortion of the body is again approximated as a second harmonic distortion, but is delayed with respect to the tide raising potential by a constant time lag. The Mignard tide is equivalent to the Darwin tide if the phase factors are taken to be proportional to frequency, and the sine of the phase lag is small enough to be approximated by the phase lag. The Mignard tides are appealing for us since they have a simple analytic form. We shall see that the frequency dependence of the tidal model is of secondary importance to correctly including all tidal interactions. An important contribution of Goldreich was the recognition that there can be average tidal effects on one body due to tides raised by an-

other body. If the spin axis is not aligned with the orbit normal, then the spin can carry the tidal bulge out of the orbital plane of the tide raising body. This out-of-plane bulge, in turn, can produce average in-plane torques on a third body. The effects due to these "cross terms" is more significant than the effects due to direct solar tides.

Goldreich expresses the tidal torques in terms of the components on one of two different sets of coordinates. One set is referred to the orbital plane of the Moon and the other is referred to the ecliptic. Denote the coordinate directions of the first system by $\hat{\mathbf{e}}_i$, and the coordinate directions of the second system by $\hat{\mathbf{f}}_i$. We have $\hat{\mathbf{e}}_3=\hat{\mathbf{b}}$, the direction perpendicular to the lunar orbit, and $\hat{\mathbf{f}}_3=\hat{\mathbf{c}}$, the normal to the ecliptic. The direction of $\hat{\mathbf{e}}_1$ is same as $\hat{\mathbf{a}}\times\hat{\mathbf{b}}$; the direction of $\hat{\mathbf{f}}_1$ is same as $\hat{\mathbf{a}}\times\hat{\mathbf{c}}$. The second coordinate directions are chosen to form a right handed system (in ascending numerical order). We write either $\mathbf{T}=T_1\hat{\mathbf{e}}_1+T_2\hat{\mathbf{e}}_2+T_3\hat{\mathbf{e}}_3$, or $\mathbf{T}=T'_1\hat{\mathbf{f}}_1+T'_2\hat{\mathbf{f}}_2+T'_3\hat{\mathbf{f}}_3$, whichever is more convenient. The projections are

$$\mathbf{T}\cdot\hat{\mathbf{a}}=T_2\sin\epsilon+T_3\cos\epsilon \tag{64}$$

$$=T'_2\sin I+T'_3\cos I, \tag{65}$$

$$\mathbf{T}\cdot\hat{\mathbf{b}}=T_3 \tag{66}$$

$$=T'_1\sin(h_0-\Omega)\sin i+T'_2\cos(h_0-\Omega)\sin i+T'_3\cos i, \tag{67}$$

$$\mathbf{T}\cdot\hat{\mathbf{c}}=T_1\left(-\frac{\sin i\sin I\sin(h_0-\Omega)}{\sin\epsilon}\right)+T_2\left(\frac{\cos I-\cos i\cos\epsilon}{\sin\epsilon}\right)+T_3\cos i \tag{68}$$

$$=T'_3. \tag{69}$$

Goldreich asserts that since all T_1 and T'_1 are multiplied by a factor of $\sin(h_0-\Omega)$ that the average of these terms is zero and thus do not need to be considered further. This is incorrect, because some T_1 and T'_1 terms are nonzero and contain an additional factor of $\sin(h_0-\Omega)$. The product has a nonzero precessional average. However, we have found that the neglected terms do not significantly affect the evolution.

2.7.1 MacDonald tides

We copy here the expressions for the average MacDonald (1964) torques from Goldreich (removing an incorrect extra factor of n):

$$T_1=0, \tag{70}$$

$$T_2=\frac{2mA}{\pi a_1^6}\frac{E(q)-q'^2K(q)}{q}\sin 2\delta, \tag{71}$$

and

$$T_3=\frac{2mA}{\pi a_1^6}q'K(q)\sin 2\delta, \tag{72}$$

with

$$A=\frac{3}{2}GmR_e^5k_2, \tag{73}$$

$$q'^2=1-q^2, \tag{74}$$

where q' has the sign of $z-\alpha$, with $\alpha=n_1/\Omega_0$, where n_1 is the mean motion of the lunar orbit, and Ω_0 is the angular rotation rate of the Earth,

$$q^2=\frac{1-\cos^2\epsilon}{1+\alpha^2-2\alpha\cos\epsilon}, \tag{75}$$

and K and E are the usual complete elliptic integrals of the first and second kind. The phase lag was taken to be 0.04635 rad. The precise value is not important here since it only sets the time scale for tidal evolution, and the actual time scale is unknown. Note that T_1 is zero, so in this case the argument about the average is moot. We do not consider solar torques or solar–lunar cross torques in the MacDonald formulation.

2.7.2 Darwin–Mignard tides

The Mignard tides are simply expressed. The torque per unit mass is

$$\mathbf{T}=-\frac{3k_2Gm^*R_e^5}{r^5r^{*5}}\Delta t\{(\mathbf{r}\times\mathbf{r}^*)[\mathbf{r}^*\cdot(\boldsymbol{\omega}\times\mathbf{r})+\mathbf{r}\cdot\mathbf{v}^*] \tag{76}$$

$$-5\frac{\mathbf{r}^*\cdot\mathbf{v}^*}{r^{*2}}(\mathbf{r}\times\mathbf{r}^*)(\mathbf{r}\cdot\mathbf{r}^*) \tag{77}$$

$$+(\mathbf{r}\cdot\mathbf{r}^*)[(\mathbf{r}\cdot\boldsymbol{\omega})\mathbf{r}^*-(\mathbf{r}\cdot\mathbf{r}^*)\boldsymbol{\omega}+\mathbf{r}\times\mathbf{v}^*]\}. \tag{78}$$

The variables with superscript * are those of the tide raising body; those without the superscript are those of the body affected by the torques.

In the case where the orbits are taken to be circular orbits the analytic averages of the Mignard torques over the orbital periods are easily accomplished. The average lunar torques due to lunar tides are

$$\mathbf{T}\cdot\hat{\mathbf{a}}=\Delta t\frac{k_2Gm_1^2R_e^5}{a_1^6}\left[\frac{3}{2}\Omega_0\sin^2\epsilon+3\cos\epsilon(\Omega_0\cos\epsilon-n_1)\right], \tag{79}$$

$$\mathbf{T}\cdot\hat{\mathbf{b}}=\Delta t\frac{k_2Gm_1^2R_e^5}{a_1^6}[3(\Omega_0\cos\epsilon-n_1)], \tag{80}$$

$$\mathbf{T}\cdot\hat{\mathbf{c}}=\Delta t\frac{k_2Gm_1^2R_e^5}{a_1^6}\left[\frac{3}{2}\Omega_0(\cos I-\cos i\cos\epsilon)+3\cos i(\Omega_0\cos\epsilon-n_1)\right]. \tag{81}$$

The average solar torques due to solar tides are

$$\mathbf{T}\cdot\hat{\mathbf{a}}=\Delta t\frac{k_2Gm_2^2R_e^5}{a_2^6}\left[\frac{3}{2}\Omega_0\sin^2 I+3\cos I(\Omega_0\cos I-n_2)\right], \tag{82}$$

$$\mathbf{T}\cdot\hat{\mathbf{b}}=\Delta t\,\frac{k_2 G m_2^2 R_e^5}{a_2^6}\left[\frac{3}{2}\,\Omega_0(\cos\epsilon-\cos I\cos i)\right.$$
$$\left.+3\cos i(\Omega_0\cos I-n_2)\right], \tag{83}$$

$$\mathbf{T}\cdot\hat{\mathbf{c}}=\Delta t\,\frac{k_2 G m_2^2 R_e^5}{a_2^6}\,[3(\Omega_0\cos I-n_2)]. \tag{84}$$

The average lunar torques due to solar tides are

$$\mathbf{T}\cdot\hat{\mathbf{a}}=\Omega_0\Delta t\,\frac{k_2 G m_1 m_2 R_e^5}{a_1^3 a_2^3}\left[\frac{3}{8}\sin^2 i\sin^2 I\cos 2(h_0-\Omega)\right.$$
$$-\frac{9}{8}\sin^2 i\sin^2 I-\frac{3}{4}\cos I\sin I\cos i\sin i$$
$$\left.\times\cos(h_0-\Omega)+\frac{3}{4}\sin^2 I\right], \tag{85}$$

$$\mathbf{T}\cdot\hat{\mathbf{b}}=0, \tag{86}$$

$$\mathbf{T}\cdot\hat{\mathbf{c}}=\Omega_0\Delta t\,\frac{k_2 G m_1 m_2 R_e^5}{a_1^3 a_2^3}\left[-\frac{3}{4}\cos i\sin i\sin I\right.$$
$$\left.\times\cos(h_0-\Omega)\right]. \tag{87}$$

The average solar torques due to lunar tides are

$$\mathbf{T}\cdot\hat{\mathbf{a}}=\Omega_0\Delta t\,\frac{k_2 G m_1 m_2 R_e^5}{a_1^3 a_2^3}\left[\frac{3}{8}\sin^2 i\sin^2 I\cos 2(h_0-\Omega)\right.$$
$$-\frac{9}{8}\sin^2 i\sin^2 I-\frac{3}{4}\cos I\sin I\cos i\sin i$$
$$\left.\times\cos(h_0-\Omega)+\frac{3}{4}\sin^2 I\right], \tag{88}$$

$$\mathbf{T}\cdot\hat{\mathbf{b}}=\Omega_0\Delta t\,\frac{k_2 G m_1 m_2 R_e^5}{a_1^3 a_2^3}\left[\frac{3}{4}\cos(h_0-\Omega)\right.$$
$$\times\sin i\sin I\cos^2 i \tag{89}$$
$$\left.-\frac{3}{4}\cos I\cos i\sin^2 i\right], \tag{90}$$

$$\mathbf{T}\cdot\hat{\mathbf{c}}=0. \tag{91}$$

Of course, the reaction torques on the Earth are the opposite of the torques on exterior bodies. The tidal time lag was taken to be about 11.54 min. Again, the precise value is not important since it sets an unknown time scale.

2.7.3 Darwin–Kaula–Goldreich tides

Goldreich focuses on the Darwin–Kaula tide with constant and equal phase lags. We record here the summed forms for these tidal torques.

The average lunar torques due to lunar tides are

$$\mathbf{T}\cdot\hat{\mathbf{a}}=\sin\epsilon_t\,\frac{k_2 G m_1^2 R_e^5}{a_1^6}\left(\frac{3}{2}-\frac{9}{16}\sin^4\epsilon\right), \tag{92}$$

$$\mathbf{T}\cdot\hat{\mathbf{b}}=\sin\epsilon_t\,\frac{k_2 G m_1^2 R_e^5}{a_1^6}\left(\frac{3}{2}\cos\epsilon+\frac{3}{4}\cos\epsilon\sin^2\epsilon\right), \tag{93}$$

$$\mathbf{T}\cdot\hat{\mathbf{c}}=\sin\epsilon_t\,\frac{k_2 G m_1^2 R_e^5}{a_1^6}\left(\frac{3}{4}\cos i\cos\epsilon\right.$$
$$+\frac{9}{16}\cos i\cos\epsilon\sin^2\epsilon \tag{94}$$
$$\left.+\frac{3}{4}\cos I+\frac{3}{16}\cos I\sin^2\epsilon\right). \tag{95}$$

The average solar torques due to solar tides are

$$\mathbf{T}\cdot\hat{\mathbf{a}}=\sin\epsilon_t\,\frac{k_2 G m_1^2 R_e^5}{a_1^6}\left(\frac{3}{2}-\frac{9}{16}\sin^4 I\right), \tag{96}$$

$$\mathbf{T}\cdot\hat{\mathbf{b}}=\sin\epsilon_t\,\frac{k_2 G m_1^2 R_e^5}{a_1^6}\left(\frac{3}{4}\cos i\cos I\right.$$
$$+\frac{9}{16}\cos i\cos I\sin^2 I \tag{97}$$
$$\left.+\frac{3}{4}\cos\epsilon+\frac{3}{16}\cos\epsilon\sin^2 I\right), \tag{98}$$

$$\mathbf{T}\cdot\hat{\mathbf{c}}=\sin\epsilon_t\,\frac{k_2 G m_2^2 R_e^5}{a_2^6}\left(\frac{3}{2}\cos I+\frac{3}{4}\cos I\sin^2 I\right). \tag{99}$$

The average lunar torques due to solar tides are

$$\mathbf{T}\cdot\hat{\mathbf{a}}=\sin\epsilon_t\,\frac{k_2 G m_1 m_2 R_e^5}{a_1^3 a_2^3}\left[\frac{3}{4}\sin^2 I-\frac{3}{8}\sin^4 I\right.$$
$$-\frac{9}{8}\sin^2 i\sin^2 I+\frac{9}{16}\sin^2 i\sin^4 I$$
$$-\frac{3}{4}\cos i\cos^3 I\sin i\sin I\cos(h_0-\Omega)$$
$$\left.+\frac{3}{16}\sin^2 i\sin^4 I\cos 2(h_0-\Omega)\right], \tag{100}$$

$$\mathbf{T}\cdot\hat{\mathbf{b}}=0, \tag{101}$$

$$\mathbf{T}\cdot\hat{\mathbf{c}}=\sin\epsilon_t\,\frac{k_2 G m_1 m_2 R_e^5}{a_1^3 a_2^3}\left[-\frac{3}{8}\cos I\sin^2 i\sin^2 I\cos 2\right.$$
$$\times(h_0-\Omega)-\left(\frac{3}{4}\cos i\sin i\sin I\right.$$
$$\left.\left.-\frac{3}{8}\cos i\sin i\sin^3 I\right)\cos(h_0-\Omega)\right]. \tag{102}$$

The average solar torques due to lunar tides are

$$\mathbf{T}\cdot\hat{\mathbf{a}}=\sin\epsilon_t\frac{k_2Gm_1m_2R_e^5}{a_1^3a_2^3}\left[\frac{3}{4}\sin^2 I-\frac{3}{8}\sin^4 I\right.$$
$$-\frac{9}{8}\sin^2 i\sin^2 I+\frac{9}{16}\sin^2 i\sin^4 I$$
$$-\frac{3}{4}\cos i\cos^3 I\sin i\sin I\cos(h_0-\Omega)$$
$$\left.+\frac{3}{16}\sin^2 i\sin^4 I\cos 2(h_0-\Omega)\right], \quad (103)$$

$$\mathbf{T}\cdot\hat{\mathbf{b}}=\sin\epsilon_t\frac{k_2Gm_1m_2R_e^5}{a_1^3a_2^3}\left[\frac{3}{4}\sin i\sin I\cos(h_0-\Omega)\right.$$
$$-\frac{3}{4}\cos i\cos I\sin^2 i-\frac{9}{8}\sin^3 i\sin I\cos(h_0-\Omega)$$
$$-\frac{3}{8}\sin i\sin^3 I\cos(h_0-\Omega)$$
$$+\frac{27}{32}\sin^3 i\sin^3 I\cos(h_0-\Omega)$$
$$+\frac{3}{4}\cos i\cos I\sin^2 i\sin^2 I$$
$$\left.-\frac{3}{32}\sin^3 i\sin^3 I\cos 3(h_0-\Omega)\right], \quad (104)$$

$$\mathbf{T}\cdot\hat{\mathbf{c}}=0. \quad (105)$$

The tidal phase lag was chosen to satisfy $\sin\epsilon_t=0.0927$. Once again, the value that would best model the tidal evolution is unknown. We have chosen the tidal constants to give similar evolutions of the semimajor axis of the lunar orbit at the present.

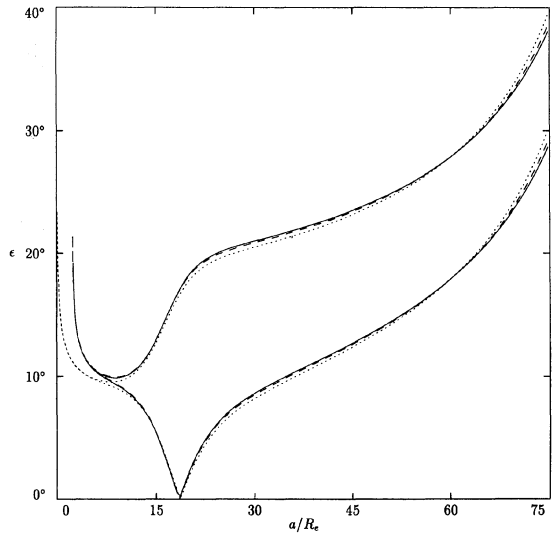

FIG. 3. The mutual obliquity ϵ is plotted vs the semimajor axis of the lunar orbit. In this and subsequent figures the evolution of a quantity is displayed by plotting the maximum and minimum over a precession period. The evolution with the average Darwin–Mignard torques is represented by the solid line, the evolution with the Darwin–Kaula–Goldreich tides with equal phase shifts is represented by the dotted line, and the evolution with the MacDonald tides are represented by the dashed line. No solar tidal contributions were included.

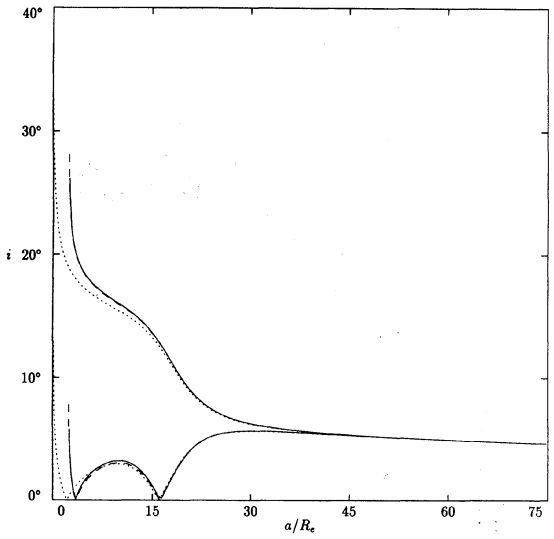

FIG. 4. The inclination of the lunar orbit i is plotted vs the semimajor axis of the lunar orbit. The evolution with the average Darwin–Mignard torques is represented by the solid line, the evolution with the Darwin–Kaula–Goldreich tides with equal phase shifts is represented by the dotted line, and the evolution with the MacDonald tides are represented by the dashed line. No solar tidal contributions were included.

2.8 Tidal Evolution

Computers are now fast enough that the integration of the equations of motion can be implemented simply and clearly. The tidal averages over the precessional period are carried

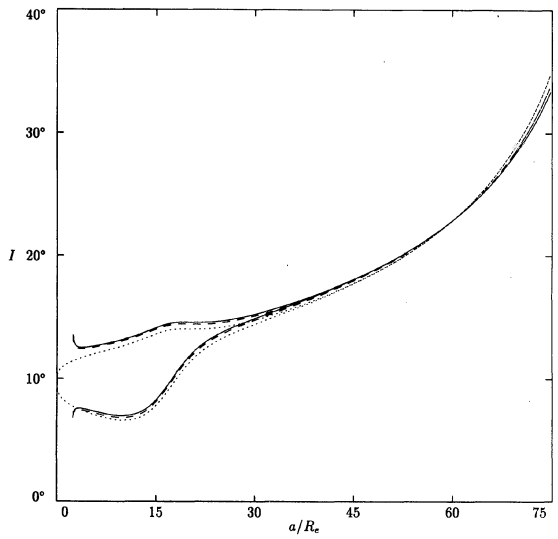

FIG. 5. The obliquity of Earth I is plotted vs the semimajor axis of the lunar orbit. The evolution with the average Darwin–Mignard torques is represented by the solid line, the evolution with the Darwin–Kaula–Goldreich tides with equal phase shifts is represented by the dotted line, and the evolution with the MacDonald tides are represented by the dashed line. No solar tidal contributions were included.

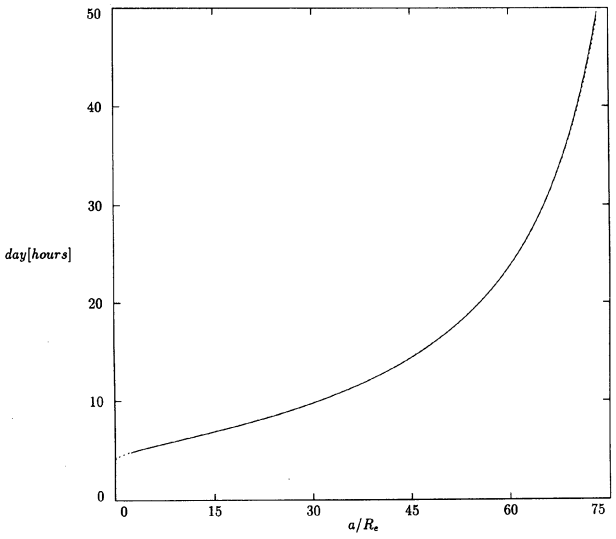

FIG. 6. The length of the day is plotted vs the semimajor axis of the lunar orbit. The evolution with the average Darwin–Mignard torques is represented by the solid line, the evolution with the Darwin–Kaula–Goldreich tides with equal phase shifts is represented by the dotted line, and the evolution with the MacDonald tides are represented by the dashed line. No solar tidal contributions were included.

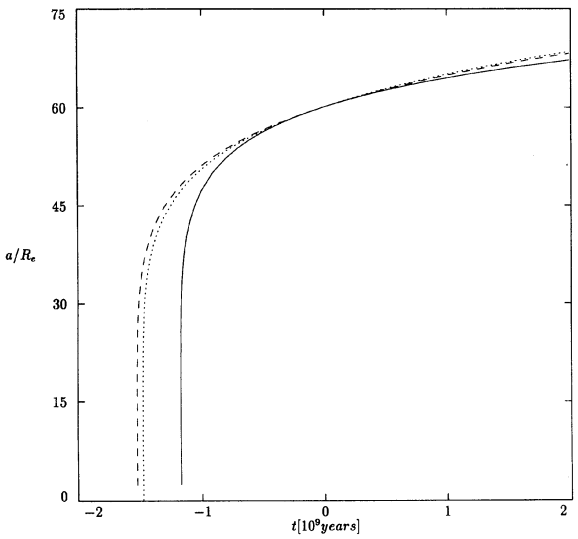

FIG. 8. The semimajor axis of the lunar orbit is plotted vs time. The evolution with the average Darwin–Mignard torques is represented by the solid line, the evolution with the Darwin–Kaula–Goldreich tides with equal phase shifts is represented by the dotted line, and the evolution with the MacDonald tides are represented by the dashed line. No solar tidal contributions were included.

out by adding extra differential equations to the precessional equations to integrate the averages for the tidal evolution. Thus, there is no extra step of integrating over a precomputed precessional trajectory as was done by Goldreich. Both the precessional evolution and the tidal evolution are computed with an implementation of the standard Bulirsch–Stoer algorithm. The relative error per step was taken to be 10^{-11}.

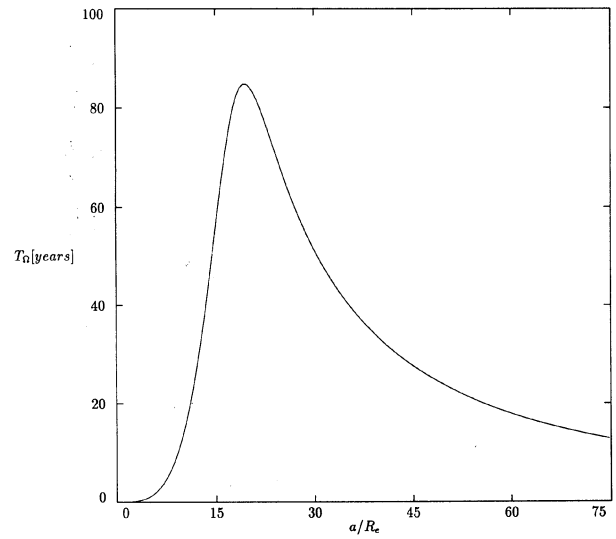

FIG. 7. The period of precession of the lunar orbit is plotted vs the semimajor axis of the lunar orbit. The evolution with the average Darwin–Mignard torques is represented by the solid line, the evolution with the Darwin–Kaula–Goldreich tides with equal phase shifts is represented by the dotted line, and the evolution with the MacDonald tides are represented by the dashed line. No solar tidal contributions were included.

2.8.1 Comparison of tidal models

We first present comparisons of the evolution of the lunar orbit with the different tidal models, including only the lunar torques due to lunar tides on the Earth. This is the only case for which we can compare all of our tidal models. Aspects of the resulting evolution are displayed in Figs. 3–8. First, our

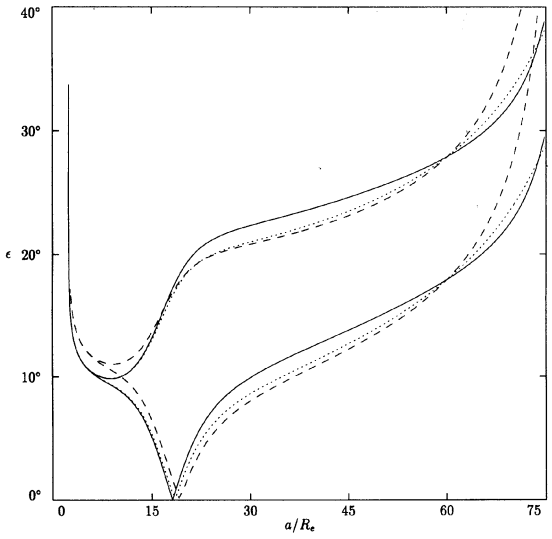

FIG. 9. The mutual obliquity ϵ is plotted vs the semimajor axis of the lunar orbit. Darwin–Mignard tides were used. The evolution with lunar tides only is represented by the dotted line, the evolution with the addition of direct solar tides is represented with the dashed line, and the solid line represents the evolution with all tidal contributions.

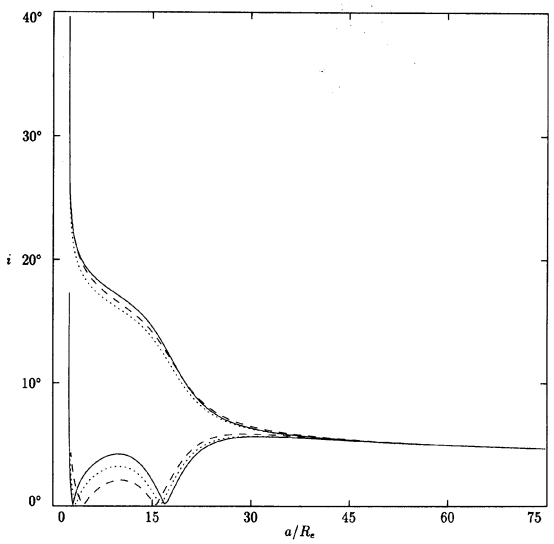

FIG. 10. The inclination of the lunar orbit i is plotted vs the semimajor axis of the lunar orbit. Darwin–Mignard tides were used. The evolution with lunar tides only is represented by the dotted line, the evolution with the addition of direct solar tides is represented with the dashed line, and the solid line represents the evolution with all tidal contributions.

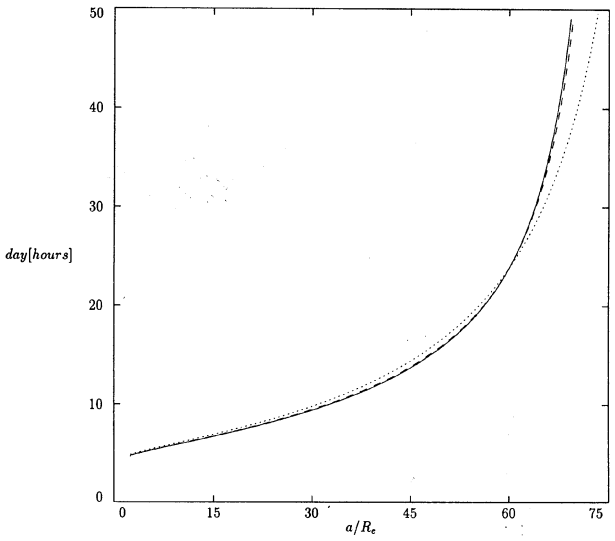

FIG. 12. The length of the day is plotted vs the semimajor axis of the lunar orbit. Darwin–Mignard tides were used. The evolution with lunar tides only is represented by the dotted line, the evolution with the addition of direct solar tides is represented with the dashed line, and the solid line represents the evolution with all tidal contributions.

formulation and implementation give evolutions which are in excellent agreement with the evolution reported in Goldreich. Also, as noted by Goldreich, the differences between the three tidal models are, for the most part, unimportant. The most important difference is that the mutual obliquity ϵ is not as large at very small lunar semimajor axes for the Darwin–Kaula–Goldreich tides as compared to the other models. The evolution of the lunar semimajor axis presents the well known time scale problem; the lunar orbit collapses only a little over a billion years ago. Presumably, the tidal constants have changed as the continents have drifted. Thus, the observed differences among models in the evolution of the semimajor axis vs time are not important. We note only that the Darwin–Mignard tides collapse faster because the tidal constants are proportional to frequency and the frequencies increase as the lunar orbit shrinks.

2.8.2 *Comparison of tidal contributions*

Next we present a comparison of the evolutions for a given tidal model with varying physical effects included

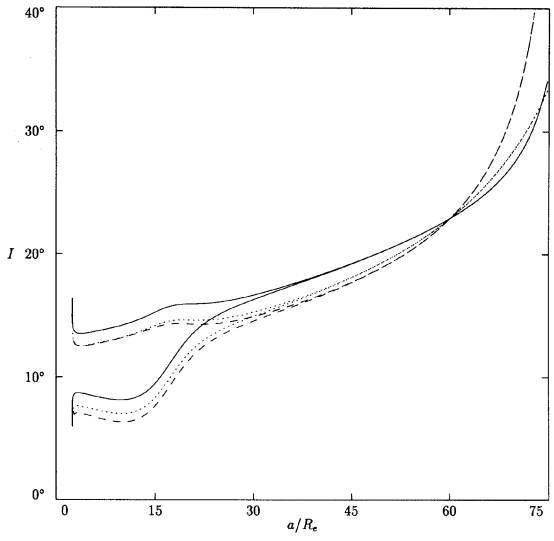

FIG. 11. The obliquity of Earth I is plotted vs the semimajor axis of the lunar orbit. Darwin–Mignard tides were used. The evolution with lunar tides only is represented by the dotted line, the evolution with the addition of direct solar tides is represented with the dashed line, and the solid line represents the evolution with all tidal contributions.

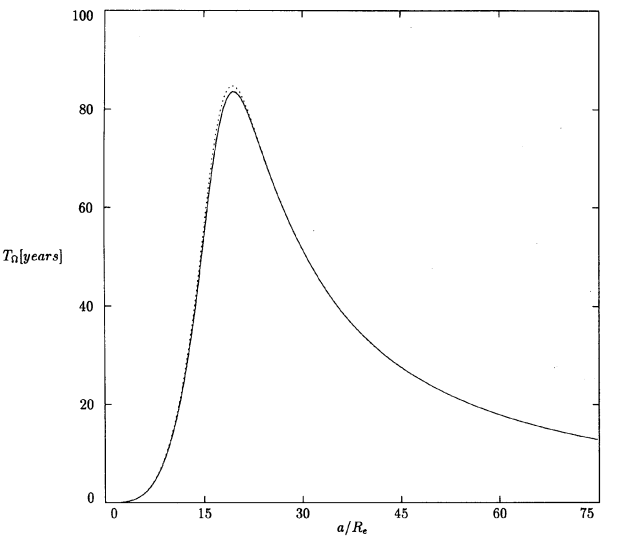

FIG. 13. The period of precession of the lunar orbit is plotted vs the semimajor axis of the lunar orbit. Darwin–Mignard tides were used. The evolution with lunar tides only is represented by the dotted line, the evolution with the addition of direct solar tides is represented with the dashed line, and the solid line represents the evolution with all tidal contributions.

(Figs. 9–14). We use the Darwin–Mignard torques. We compare the evolution with lunar tides only, lunar tides plus direct solar tides, and lunar tides with direct and indirect solar tides. Here the differences are more pronounced than in the last set of comparisons. Thus, it is more important to correctly incorporate all the effects than it is to have the correct tidal model. Note that the direct solar torques typically have the opposite effect as the indirect cross terms, and that the cross terms seem to be more important, as reported by Goldreich.

2.8.3 Comparison of full models

Finally, we present evolutions computed with the Darwin–Kaula–Goldreich torques and the Darwin–Mignard torques, with all tidal effects included (Figs. 15–20). These two models both include all the torques and cross torques, but differ by the frequency dependence of the torques.

The agreement of our calculation using Darwin–Kaula–Goldreich tides with the calculation by Goldreich is not bad, but not perfect either. The origin of the discrepancy is unknown; however, we have checked that it is not due to Goldreich's omission of T_1 and T_1' terms.

These two models exhibit very similar evolution in the past. The inclusion of cross terms and solar torques has a much larger effect than changing the frequency dependence of the tidal torques. In the future, the obliquity of the Earth increases less rapidly in the constant tidal phase model than in the model with frequency dependent phases.

A principal result of Goldreich's paper was that the mutual obliquity of the lunar orbit to the Earth's equator is large at small lunar semimajor axes. All of our models confirm this result, though the evolution is different in detail. We are presented with an unresolved mystery. All theories of lunar formation require that formation take place in the equator plane, yet models of tidal evolution do not place the Moon there.

3. INCORPORATION OF TIDAL FRICTION INTO THE SYMPLECTIC INTEGRATION SCHEME

At this point, we leave the simple, but revealing model of Goldreich, and move on to examine the tidal evolution of the Earth–Moon system numerically. We are anxious to relax the assumptions that were introduced earlier.

3.1 What a Mess: Ad Hoc Models of Tides

In our search for a physically plausible model of tidal interactions, it was natural to consider the road taken by ephemeris calculators. We considered a paper on the DE 102 ephemeris written by Newhall *et al.* (1983). DE 102, "a numerically integrated ephemeris of the Moon and planets spanning 44 centuries," used the following expression for the tidally induced geocentric acceleration of the Moon:

$$\ddot{\mathbf{r}}_{\text{tides}}=\frac{-3k_2\mu_m}{r_{em}^3}\left(1+\frac{\mu_m}{\mu_e}\right)\left(\frac{R_e}{r_{em}}\right)^5\begin{bmatrix}x+y\,\delta\\ y-x\,\delta\\ z\end{bmatrix}, \tag{106}$$

where k_2 is the potential Love number of the Earth; δ is the phase lag of the tidal bulge raised by the Moon on the Earth; μ_e is the gravitational constant times the mass of the Earth; μ_m is the gravitational constant times the mass of the Moon; R_e is the radius of the Earth; r_{em} is the geocentric lunar distance; x, y, and z are the components of the geocentric position vector of the Moon expressed in the "true-of-date system." Since DE 102 does not integrate the Earth rotation, a true-of-date coordinate system is obtained by performing the "necessary" orthogonal transformations on the reference coordinate system.

The assumptions that go into deriving this expression for the tides were not discussed in the DE 102 paper. However, the authors referred to a paper by Williams *et al.* (1978) "for further discussion." The latter paper writes the same expression but again with very little explanation:

Mathematically a "tidal bulge" is raised by adding a term to the potential of the Earth which is proportional to the potential Love number k_2 and the second degree Legendre polynomial P_2. The symmetry axis of this bulge is then rotated forward (right handed) about the spin axis of the Earth by a phase angle δ.

Instead of trying to make direct sense of the DE 102 tidal accelerations, we decided to work with Mignard's tidal model. In our study of the multiply averaged theory just presented, we found that the frequency dependence of the tidal model was less important than including all the physical effects. In particular, we found that the averaged Darwin–Mignard torques gave very similar evolution to the averaged Darwin–Kaula–Goldreich torques. We adopt the Mignard's model for our numerical work because it is analytically simpler. Starting with the Mignard tides we can understand the constraints that have to be applied in order to recover the DE 102 tidal accelerations. These constraints demonstrate why the DE 102 model of tides is not applicable to the Earth–Moon system in long (and perhaps short) term integrations.

So without further archeology, we proceed to discuss in more detail the tidal model used by Mignard. Instead of a constant phase delay δ in the tidal response, Mignard assumes a constant time delay Δt and then Taylor expands the delayed dynamic variables, assuming a small Δt.

The tide raising potential can be expanded in the usual way in terms of Legendre polynomials. We consider the second order term in the potential:

$$U_0=\frac{\mu_p}{2r_p^5}\left[3(\mathbf{r}\cdot\mathbf{r}_p)^2-r^2r_p^2\right], \tag{107}$$

where μ_p is the gravitational constant times the mass of the tide raising body; $\mathbf{r}_p$ is the position vector of the tide raising body; $\mathbf{r}$ is the point where the potential is calculated. The tide raising potential produces an elastic deformation of the Earth which leads to an additional potential at position $\mathbf{r}$ given by

$$U(\mathbf{r})=k_2\frac{\mu_pR_e^5}{2r_p^5r^5}\left[3(\mathbf{r}\cdot\mathbf{r}_p)^2-r^2r_p^2\right], \tag{108}$$

where as before k_2 is the potential Love number of the Earth and R_e is the radius of the Earth. This form of the potential

holds in case the elastic deformation of the body is ideal. In the presence of dissipation, we assume, with Mignard, that the tidal response is delayed by a time Δt which is small compared to the rotational and the orbital frequencies in the problem. Thus, the additional potential at time t, evaluated at position $\mathbf{r}(t)$, is equal to the additional potential produced by an ideal response of the Earth with the perturbing body at $\mathbf{r}_d(t)=\mathbf{r}_p(t-\Delta t)+\boldsymbol{\omega}(t)\times\mathbf{r}_p(t-\Delta t)$. If we expand $\mathbf{r}_d$ for small Δt we find

$$\mathbf{r}_d(t)=\mathbf{r}_p(t)-\Delta t\mathbf{v}_p(t)+\boldsymbol{\omega}(t)\times\mathbf{r}_p(t), \tag{109}$$

where $\mathbf{v}_p(t)$ is the velocity of the perturbing body at time t. Next, we carry out the following steps: (1) replace $\mathbf{r}_p$ in U by the approximate expression for $\mathbf{r}_d$; (2) expand the potential up to terms of order Δt; (3) find the additional force at $\mathbf{r}$ due to a perturber at $\mathbf{r}_p$ by taking the gradient of the potential energy with respect to $\mathbf{r}$; (4) equate $\mathbf{r}$ to $\mathbf{r}_p$ in the expression of the force to find the force experienced by the perturbing body (the Moon) due to the deformations it produces on the Earth.

We recover the force acting on the Moon due to a delayed tidal bulge on the Earth:

$$\mathbf{F}_{\text{tides}}=-\frac{3k_2GM_m^2R_e^5}{r_{em}^{10}}\{r_{em}^2\mathbf{r}_{em}+\Delta t[2\mathbf{r}_{em}(\mathbf{r}_{em}\cdot\mathbf{v}_{em})+r_{em}^2(\mathbf{r}_{em}\times\boldsymbol{\omega}+\mathbf{v}_{em})]\}. \tag{110}$$

The tidal torque acting on the lunar orbit is given by

$$\mathbf{T}=\mathbf{r}_{em}\times\mathbf{F}=-\frac{3k_2GM_m^2R_e^5\Delta t}{r_{em}^{10}}\times[(\mathbf{r}_{em}\cdot\boldsymbol{\omega})\mathbf{r}_{em}-r_{em}^2\boldsymbol{\omega}+\mathbf{r}_{em}\times\mathbf{v}_{em}]. \tag{111}$$

An equal and opposite torque acts on the Earth figure. We finally give an expression for the geocentric tidal acceleration of the Moon:

$$\ddot{\mathbf{r}}_{\text{tides}}=-\frac{3k_2\mu_m\left(1+\frac{\mu_m}{\mu_e}\right)R_e^5}{r_{em}^{10}}\{r_{em}^2\mathbf{r}_{em}+\Delta t[2\mathbf{r}_{em}(\mathbf{r}_{em}\cdot\mathbf{v}_{em})+r_{em}^2(\mathbf{r}_{em}\times\boldsymbol{\omega}+\mathbf{v}_{em})]\}. \tag{112}$$

Similar expressions can be derived for the cross terms by taking the derivative with respect to the unstarred variables and keeping the starred variables in the equations.

Under what conditions do we recover the DE 102 expression? First, we decouple the Earth rotation from the tidal interaction: $\boldsymbol{\omega}=\omega\mathbf{k}$, where ω is the angular velocity of the Earth, and $\mathbf{k}$ is a unit vector along the z axis of the Earth. Second, we assume an equatorial circular orbit for the Moon: $\mathbf{v}_{em}=n\mathbf{k}\times\mathbf{r}_{em}$, where n is the orbital mean motion. After enforcing these constraints, the tidal acceleration becomes

$$\ddot{\mathbf{r}}_{\text{tides}}=-\frac{3k_2\mu_m\left(1+\frac{\mu_m}{\mu_e}\right)R_e^5}{r_{em}^8}[\mathbf{r}_{em}+\Delta t(\omega-n)\mathbf{r}_{em}\times\mathbf{k}]. \tag{113}$$

Setting $\delta=\Delta t(\omega-n)$, we recover the DE 102 expression.

A few remarks are in order. The Moon's orbit is of course neither equatorial, nor circular, nor even elliptical. This model of the tides doesn't apply to the Moon. Assuming we were to ignore the eccentricity of the Moon, the misalignment of the angular momenta of the lunar orbit and the Earth is not negligible. An expression which would take that factor into account is given by

$$\ddot{\mathbf{r}}_{\text{tides}}=-\frac{3k_2\mu_m\left(1+\frac{\mu_m}{\mu_e}\right)R_e^5}{r_{em}^8}\times[\mathbf{r}_{em}+\Delta t\mathbf{r}_{em}\times(\omega\mathbf{k}-n\mathbf{k}_0)], \tag{114}$$

where $\mathbf{k}_0$ is a unit vector normal to the plane of the circular lunar orbit. This expression is, however, not general enough for our purposes. We use the more general expressions derived above.

4. THE MESS IN TIME: TIDES AND INTEGRATORS

We have derived Lie–Poisson integrators for rigid body dynamics in the solar system (Touma & Wisdom 1994). These integrators follow the free rigid body dynamics, the Keplerian motion, point–point interactions and body–point interactions. The algorithms preserve the symplectic structure and the total angular momentum of the system. Dissipation will affect the symplectic structure, but the total angular momentum should remain constant.

Emphasizing the conservation properties of the dynamics, we can write the differential equations in the following manner:

$$\frac{d}{dt}\mathbf{x}=\mathbf{v}_H+\mathbf{v}_D, \tag{115}$$

where $\mathbf{v}_H$ denotes the Hamiltonian vector field of the conservative dynamics, and $\mathbf{v}_D$ denotes the dissipative vector field. The derivation of our symplectic algorithms relies on the averaging principle and the Hamiltonian nature of the dynamics. However, if we focus on the maps as integrators then they are clearly applicable to the approximation of general vector fields, whether or not they are Hamiltonian. So whatever algorithm we use to integrate the Hamiltonian vector field, we can write

$$\mathbf{x}(t)=\exp(\mathbf{v}_H+\mathbf{v}_D t)\mathbf{x}(0)=\exp(\mathbf{v}_H t)\exp(\mathbf{v}_D t)\mathbf{x}(0)+O(t^2). \tag{116}$$

Of course, higher order approximations of the dynamics can be obtained in the usual fashion. The first order splitting corresponds to the intuitive idea of a dissipative kick to the conservative dynamics.

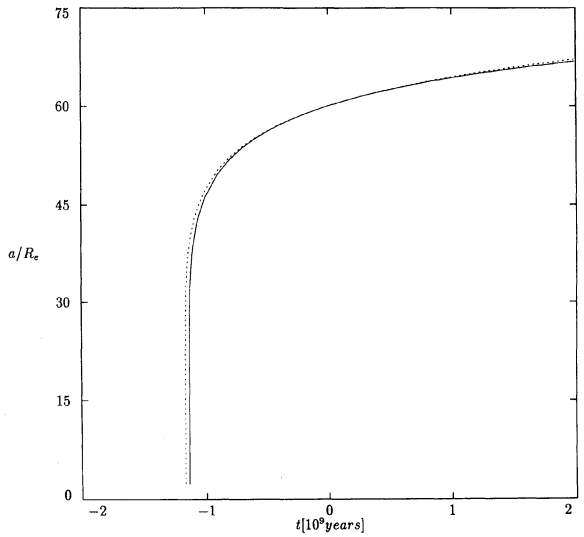

FIG. 14. The semimajor axis of the lunar orbit is plotted vs time. Darwin–Mignard tides were used. The evolution with lunar tides only is represented by the dotted line, the evolution with the addition of direct solar tides is represented with the dashed line, and the solid line represents the evolution with all tidal contributions.

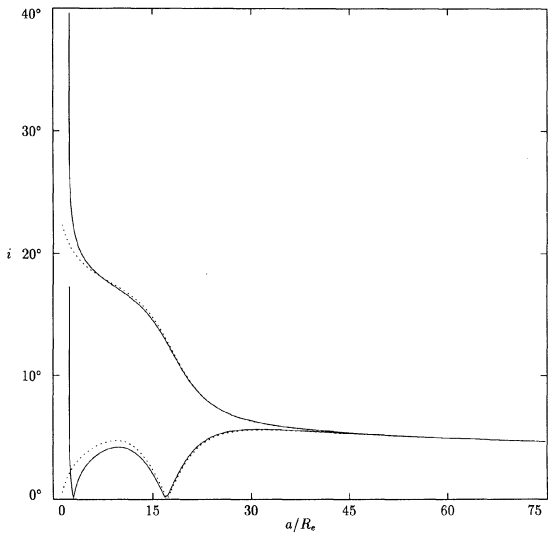

FIG. 16. The inclination of the lunar orbit i is plotted vs the semimajor axis of the lunar orbit. The evolution with the average Darwin–Mignard torques is represented by the solid line, and the evolution with the Darwin–Kaula–Goldreich tides with equal phase shifts is represented by the dotted line. All tidal effects are included.

Having dealt with the Hamiltonian contributions in Touma & Wisdom (1994), we briefly discuss the dissipative effects. The dissipative kicks, given by Eqs. (111) and (112) act at a fixed radius, and depend linearly on the momenta. The integral curves are given by the exponential of a constant matrix. In our calculations, we found it well within the order of the integration to keep the first two terms in the Taylor expansion of the solution. Explicitly, over a time step Δt, the tide raised by the Moon on the Earth kicks the spin angular momentum of the Earth by

$$\Delta \mathbf{L}_{\text{Earth}} = \mathbf{T}\Delta t, \tag{117}$$

and the geocentric velocity of the Moon by

$$\Delta \mathbf{v}_{em} = \ddot{\mathbf{r}}_{\text{tides}}\Delta t, \tag{118}$$

where $\mathbf{T}$ and $\ddot{\mathbf{r}}_{\text{tides}}$ are the torque and geocentric acceleration vectors, given by Eqs. (111) and (112). These vectors are evaluated at the current geocentric position and velocity vectors of the Moon and the current angular velocity vector of

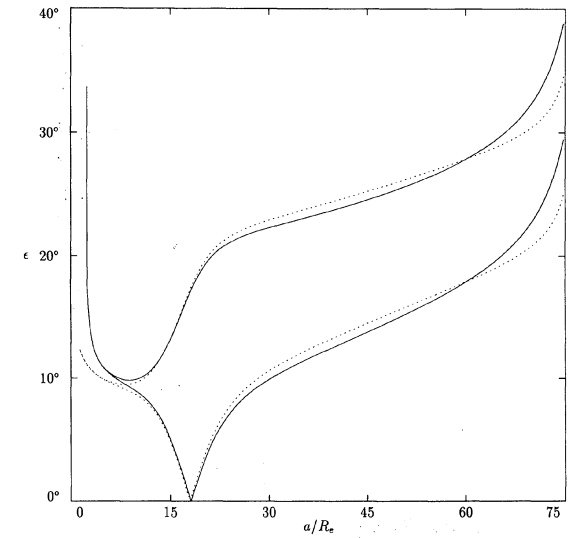

FIG. 15. The mutual obliquity ϵ is plotted vs the semimajor axis of the lunar orbit. The evolution with the average Darwin–Mignard torques is represented by the solid line, and the evolution with the Darwin–Kaula–Goldreich tides with equal phase shifts is represented by the dotted line. All tidal effects are included.

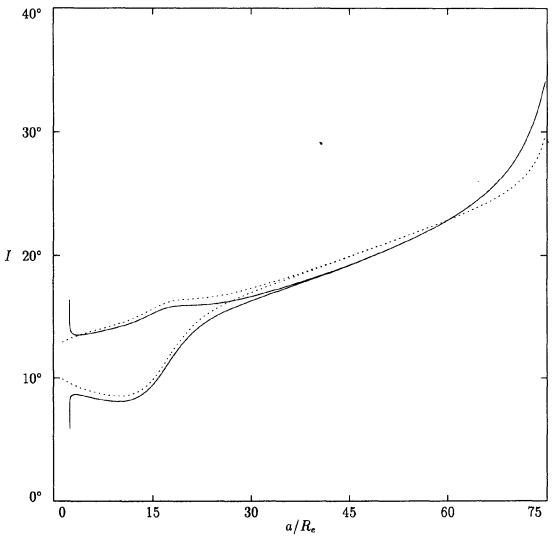

FIG. 17. The obliquity of Earth I is plotted vs the semimajor axis of the lunar orbit. The evolution with the average Darwin–Mignard torques is represented by the solid line, and the evolution with the Darwin–Kaula–Goldreich tides with equal phase shifts is represented by the dotted line. All tidal effects are included.

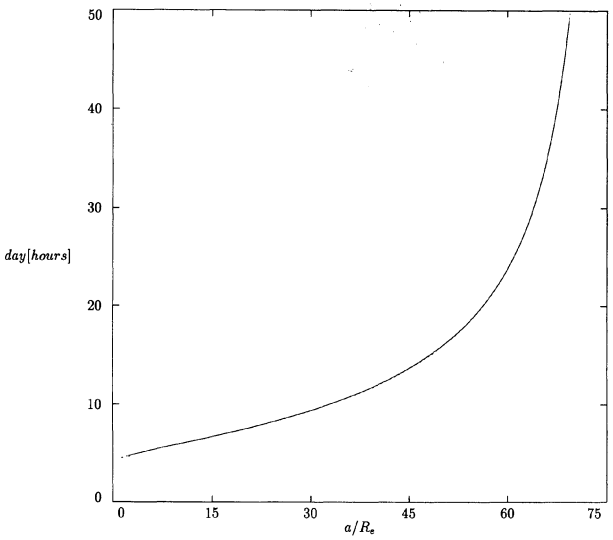

FIG. 18. The length of the day is plotted vs the semimajor axis of the lunar orbit. The evolution with the average Darwin–Mignard torques is represented by the solid line, and the evolution with the Darwin–Kaula–Goldreich tides with equal phase shifts is represented by the dotted line. All tidal effects are included.

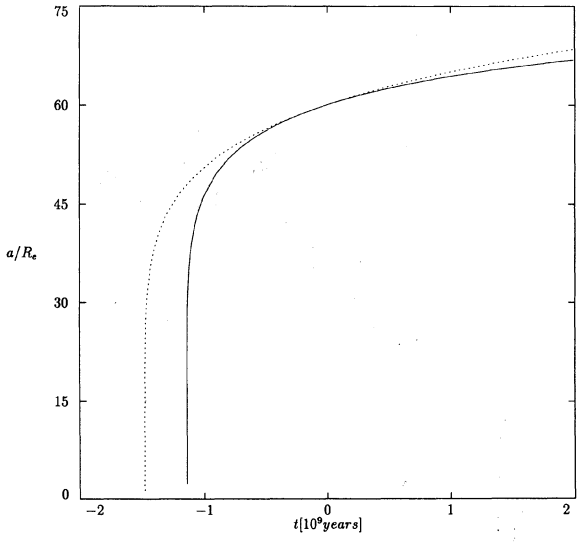

FIG. 20. The semimajor axis of the lunar orbit is plotted vs time. The evolution with the average Darwin–Mignard torques is represented by the solid line, and the evolution with the Darwin–Kaula–Goldreich tides with equal phase shifts is represented by the dotted line. All tidal effects are included.

the Earth. Kicks due to solar tides and cross tidal interactions can be similarly applied.

Another consequence of the dissipation is the change in J_2 that results from the changing spin rate of the Earth. We take account of this change by updating J_2 after each cycle of the full integrator. We apply the Hamiltonian and dissipative kicks as if the tensor of inertia were constant in time, then use the resulting spin angular velocity of the Earth to update J_2 via Eq. (56). We neglected off-diagonal contributions to the tensor of inertia, mostly because, in our simulations, the Earth did not develop a substantial wobble.

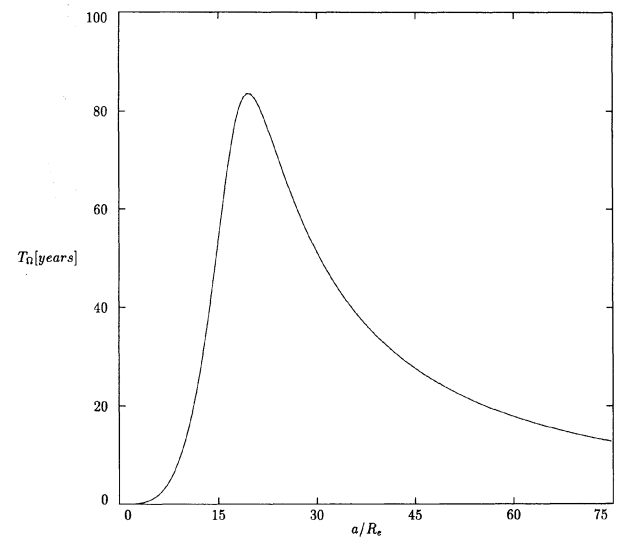

FIG. 19. The period of precession of the lunar orbit is plotted vs the semimajor axis of the lunar orbit. The evolution with the average Darwin–Mignard torques is represented by the solid line, and the evolution with the Darwin–Kaula–Goldreich tides with equal phase shifts is represented by the dotted line. All tidal effects are included.

5. PAST EVOLUTION OF THE EARTH–MOON SYSTEM

Equipped with our integrator, we proceed to examine the tidal evolution of the Earth–Moon system. We consider a Moon which interacts gravitationally with the rest of the solar system. We keep only the J_2 term in the potential of the Earth. We include dissipation in the Earth, and we allow tides to be raised by both the Sun and the Moon, and account for cross-tidal effects. We ignore dissipation in the Moon because the rotational dynamics of the Moon presented some complications which we will address in a separate paper. The model as it stands is detailed enough to allow comparison with existing calculations of the rotation of the Earth and the history of the Earth–Moon system. Furthermore, it is flexible enough to allow extensions to more detailed models of elasticity and dissipation.

5.1 Physical Parameters

The initial position and velocity of the planets and the Moon are those of DE202. The initial orientation of the spin axis of the Earth was derived using the formulas in Davies *et al.* (1989). The initial dynamical ellipticity was chosen, in the usual manner, to provide the observed general precession rate of the Earth: J_2=0.003 267 11. We delayed the tidal bulge raised by the Moon on the Earth by a phase that reflects the current tidal dissipation rate: Δt=0.006 918 25 days.

5.2 Obliquity of the Earth over the Past 20 Million Years

We examine the evolution of the Earth–Moon system in the past 20 Myr. The results of our calculated obliquity are

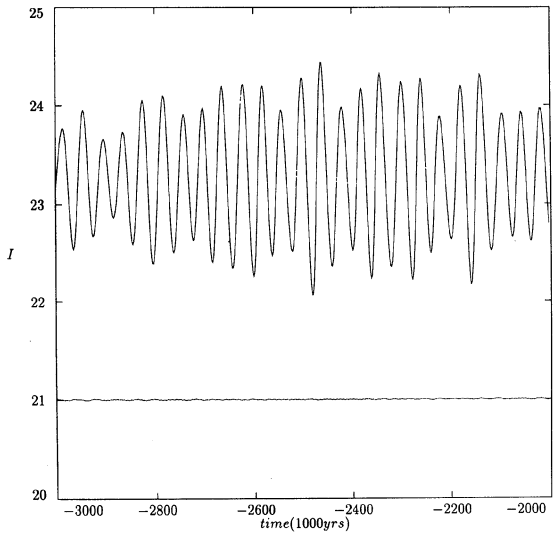

FIG. 21. The solution of the obliquity in this paper is superposed on the solution of QTD. They are almost indistinguishable. The difference is plotted on the same graph.

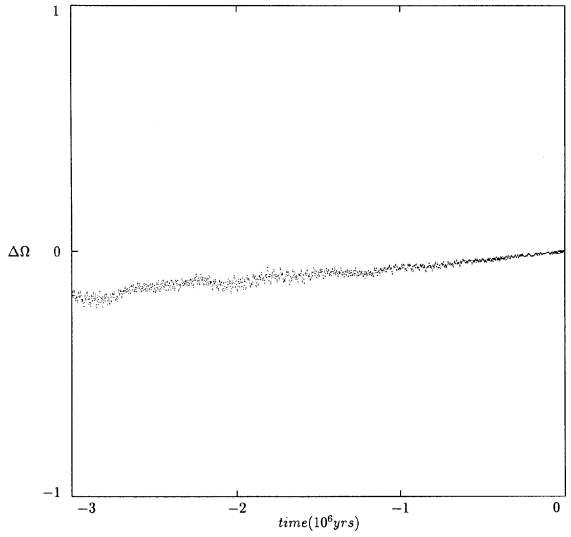

FIG. 22. The Equinox calculated in this paper differs from the QTD Equinox by a tenth of a degree after 3 Myr.

shown in Fig. 23. We compared our results to those of Quinn *et al.* (1991, hereafter referred to as QTD) who calculated the orbital evolution of the planets and the spin axis of the Earth for the past 3 Myr. Our model differs from that of QTD. Our Moon is a tidally evolving particle interacting with the planets and the Earth oblatness; their Moon is a ring in the plane of the ecliptic with a tidally evolving radius. Our tidal model is coupled to the dynamics of the Earth orbit and spin state; their tidal model consists of a linear evolution of the spin rate of the Earth and the radius of the Moon. We find that after 3 Myr of the evolution our calculated obliquity is virtually indistinguishable from theirs, Fig. 21. The equinox, shown in Fig. 22, shows a difference of a tenth of a degree after the same period of time. This result provides an independent check on the QTD model, as it demonstrates the accuracy of our algorithm. With our confidence strengthened, we move on to examine the long term evolution of the Earth–Moon system where QTD's model is no longer valid and where our model should capture most of the relevant dynamics.

5.3 Goldreich Revisited

Despite the algorithmic improvements introduced in this paper, and despite the gain in computer speed, a full history of the Earth–Moon system with the current dissipation rates will have to wait for a year. Instead, during the slow phase of the evolution, 60 to 30 Earth radii, we increased the dissipation rate in the Earth to 4000 times its current value, and set it back to 100 times its current value before 30 Earth radii where the dissipation is much more efficient. Further attention should be given to the possibility that resonances have been missed during this evolution.

Our calculations do not show any fundamental departures from the Goldreich picture. In particular, the inclination of the lunar orbit to the Earth's equator remains large at small lunar semimajor axis. As can be seen in Figs. 24–27, the averaged evolution of the relevant dynamical variables is preserved, with high frequency oscillatory features superposed on it. It was sobering to find, a few decades after its inception, that Goldreich's brush stroke captured the essence of the dynamics.

Close to the Earth, the graphs are multivalued because in the final stage of its evolution, the Moon receeds from the Earth on a highly inclined orbit, until it finally escapes. This behavior is a reminder of the lively dynamics of the early evolution of the Earth–Moon system. These dynamics are still not properly represented in our model. As pointed out by Boss & Peale (1986), the early evolution of the Earth–Moon system is characterized by intense deformations, which are poorly modeled by a quasistatic tidal bulge, and which could lead to drastically different dynamics. Thus, the model stud-

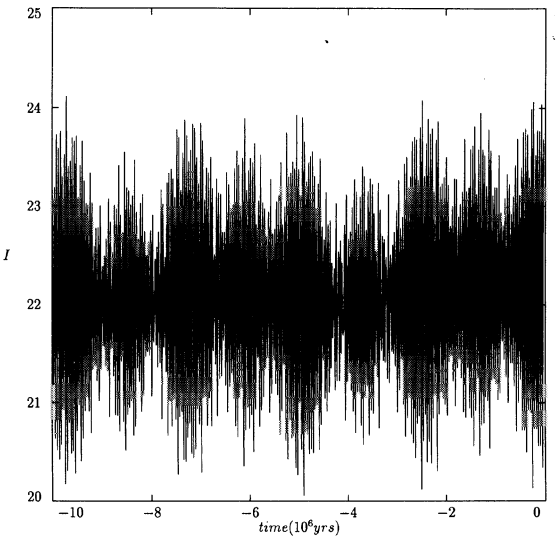

FIG. 23. The obliquity of the Earth for the last 20 Myr.

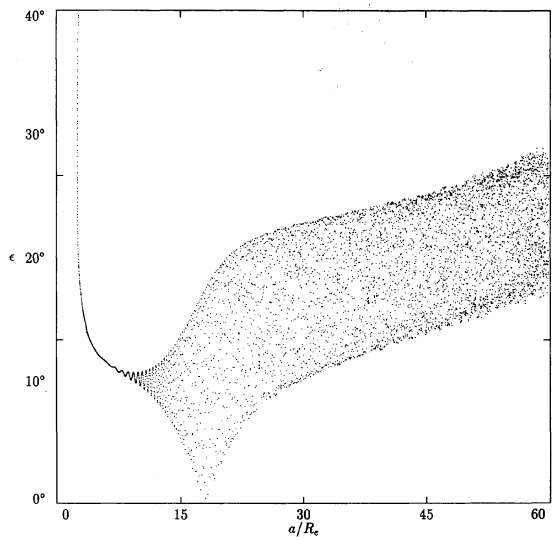

FIG. 24. The mutual obliquity is plotted vs the semimajor axis of the orbit.

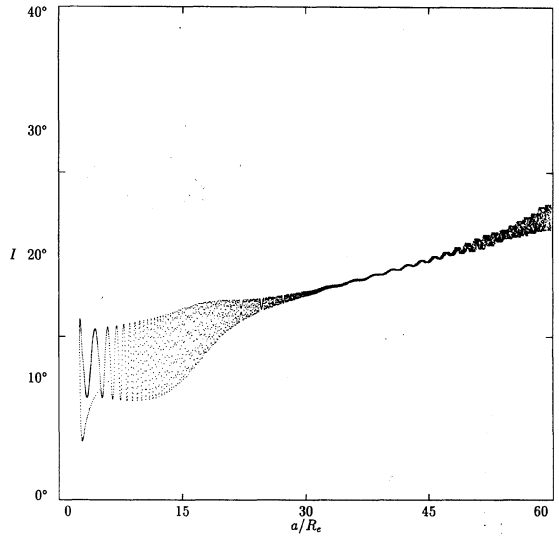

FIG. 26. The obliquity is plotted vs the semimajor axis of the orbit.

ied in this paper cannot provide a dynamical constraint on the origin of the Moon. Rather, our success in reproducing results of the averaged theory makes a case for our algorithm as a building block of a more realistic model of the early dynamics of the Earth–Moon system, as well as a tool for examining the tidal evolution of planetary satellites in general.

6. WHAT'S UP?

We have developed an accurate and efficient numerical algorithm which allows the exploration of long term consequences of tidal dissipation on the orbital and rotational dynamics of planets and their satellite(s). In doing so, we are a step closer to a realistic modeling of the evolution of the solar system. However, with regard to the Earth–Moon system, important steps remain to be taken in order to better represent the dynamics. On the short term, the coupling between climate and rotation deserves attention and our algorithm offers a secure building ground. On the long run, we need to include dissipation in the Moon. This step is complicated by the artificial excitation of wobble in the Moon as we integrate backwards in time and by the early instability of the Moon's spin axis that was first studied by Ward (1982). Both of these issues will be addressed in a companion paper. Finally, the elastic response we used in this paper is linear, quasistatic and is expected to break down in the early evolution of the Earth–Moon system. One can partially improve this picture by modeling the Earth and the Moon as pseudorigid bodies with viscoelastic material properties, thus allowing a more intrinsic coupling between elastic deformation and rotation.

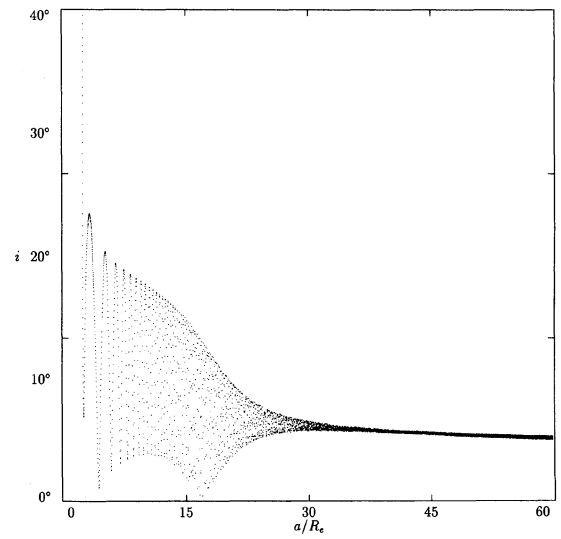

FIG. 25. The inclination of the lunar orbit to the ecliptic is plotted vs the semimajor axis of the orbit.

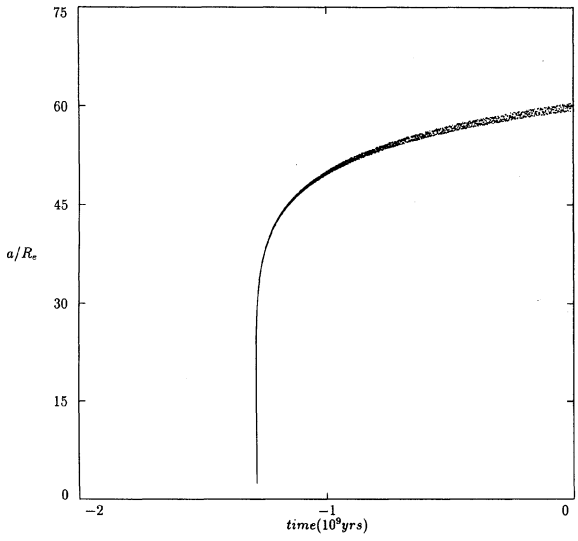

FIG. 27. The semimajor axis of the lunar orbit is plotted vs time.

This research had its origin in a research seminar at MIT on the dynamics of the lunar orbit which brought together the authors with Gerald Sussman, Matt Holman, and Kathy Olkin. The research was supported in part by the NASA Planetary Geology and Geophysics Program under Grant No. NAGW-706, and by an NSF Presidential Young Investigator Award, AST-8857365. Jihad Touma expresses his gratitude to the staff of the Lunar and Planetary Institute for their hospitality while the project was being completed.

REFERENCES

Allen, C. W. 1973, Astrophysical Quantities (Athlone, London)
Andoyer, H. 1923, Cours de Mechanique Celeste, Vol. 1 (Gauthier-Villars, Paris)
Boss, A. P., & Peale, S. J. 1986, in Origin of The Moon, edited by W. K. Hartmann, R. J. Phillips, and G. J. Taylor (Lunar and Planetary Institute, Houston), p. 59
Burns, J. A. 1986, in Satellites, edited by J. A. Burns and M. S. Matthews (University of Arizona Press, Tucson), p. 117
Darwin, G. H. 1880, PTRSL, 171, 713
Davies, M. E., *et al.* 1989, Celestial Mechanics, 46, 187
Goldreich, P. 1966, Rev. Geophys., 4, 411
MacDonald, G. J. F. 1964, Rev. Geophys., 2, 467
Mignard, F. 1981, Moon and Planets, 24, 189
Newhall, X. X., Standish, E. M., & Williams, J. G. 1983, A&A, 125, 150
Quinn, T. R., Tremaine, S. D., & Duncan, M. 1991, AJ, 101, 2287
Touma, J., & Wisdom, J. 1993, Science, 259, 1294
Touma, J., & Wisdom, J. 1994, AJ, 107, 1189
Ward, W. R. 1982, Icarus, 50, 444
Williams, J. G., Sinclair, W. S., & Yoder, C. F. 1978, Geophys. Res. Lett., 5, 943
Wisdom, J., & Holman, M. 1991, AJ, 102, 1528